TÉCNICO LISBOA

Bacterial Growth in the Presence of Several Resources

Ana Rita Gonçalves

Thesis to obtain the Master of Science Degree in

Engineering Physics

Supervisors:
Doutora Isabel Antunes Mendes Gordo
Prof. Doutor Rui Manuel Agostinho Dilão

Examination Committee

Chairperson: Ilídio Pereira Lopes
Supervisor: Prof. Doutor Rui Manuel Agostinho Dilão
Member of the Committee: Doutor Paulo Jorge Rêgo Durão

July 2020

Resumo analítico

Existem diversos modelos que descrevem a dinâmica de uma população na presença de recursos. Atualmente, os modelos desenvolvidos têm bases empíricas, sendo a mais comum o modelo do Monod, e não incluem a descrição de alguns fenómenos importantes.

Motivados pela falta de bases nos modelos existentes, apresentamos alternativas de complexidade sucessiva, com base nos processos biológicos conhecidos e que reproduzem os comportamentos observados, tentando establecer uma conexão entre a teoria e observações experimentais.

Analisámos dados retirados de diferentes experiências e também de experiências desenhadas e executadas por nós no Instituto Gulbenkian de Ciência, usando culturas de *E. coli* para observar o crescimento bacteriano sob diferentes condições e avaliar o ajuste dos modelos.

As simulações que apresentamos, feitas com os nossos modelos, apontam para o facto de que a função Monod pode servir de boa aproximação a algumas experiências mas não é o modelo correcto, embora sejam necessários mais testes para podermos validar ou discartar totalmente os nossos modelos.

Propomos uma experiência em que o crescimento bacteriano e a concentração de nutrientes sejam medidos em separado, com a intenção de os calibrar usando os modelos matemáticos aqui desenvolvidos, e relacionar tal como foi feito com os dados experimentais do Mostovenko.

Palavras-chave:
E. coli, mitose, diauxias, densidade óptica, estratégias metabólicas, *trade-off*.

Abstract

There are several models describing the dynamics of a population in the presence of resources. Currently, these models are based on empirical foundations, most commonly the Monod's model, and fail to include some core phenomena.

Motivated by the lack of foundation on the existent models, we present alternatives with increasing complexity and basis on the known biological processes that do reproduce the observed behaviors, aiming to establish a connection between the theory and empirical observations.

We analyze data collected from different experiments and also from experiments designed and executed by us at Instituto Gulbenkian de Ciência using cultures of *E. coli* to observe the bacterial growth in different conditions and to find the fitting of the models. The simulations we present, done with our models, point to the fact that the Monod function may be a good approximation to some experiments but not the correct model, although further tests need to be done in order to fully validate or discard our models.

We propose an experiment where the bacterial growth and nutrient concentrations are measured separately, with the intention of calibrating them using the models here developed, and relating the two as done with the Mostovenko's experimental data.

Key-words:
E. coli, mitosis, diauxies, optical density, metabolic strategies, trade-off.

Contents

List of Figures

Nomenclature

k	Kinetic rates / coefficients
C	Carrying Capacity
P	Amount of protein produced
β	Index of species
B	Number of different species
N_β	Number of individuals of the species β
U_β	Maximum Uptake rate of the species β
δ_β	Death rate of the species β
M_β	Resource-population mass conversion factor
i	Index of individuals of a population
N	Total Number of individuals
n	Population density
g	Normalized growth rate
j	Type of resource
J	Number of resource types
R_j	Amount of Resource of type j
w_j	Weight parameter = importance of nutrient type i
v_j	Nutritional value of the nutrient type j
R_j^T	Threshold of resource of type j
s_j	Supply rate of nutrient of type j
A_j	Availability of resources of type j
d_j	Degradation rate of nutrients of type j
$p_{\beta j}$	Probability of individual of species β finding and consuming nutrient of type j
$\alpha_{\beta j}$	Metabolic strategies = consumption rate of j by β
G	Glucose
S	Sorbitol
E	Enzyme
X	Nutrient-enzyme complex
D	Product of Death
γ	Generation

Chapter 1

Introduction and State of the art

It is currently estimated that there are more than 10 million different species on our planet, [1]. This incredible biodiversity has been captivating scientists since the 20th century.

Living beings interact with other beings of the same species and of different species in order to feed themselves (predation), cooperate (mutualism) or fight for the same resources (competition). These interactions give rise to a highly complex network that governs the population dynamics and determine whether they lead to the species' coexistence or extinction. It is therefore a great challenge to understand how it is possible for such a vast number of species to coexist in equilibrium and how stable this equilibrium is.

We know that species have the ability to adapt to changes in the environment, [2], but the connection between this phenomenon and the existing populational models is still missing. Biologically and mathematically we are still far from fully understanding on how adaptative evolution works.

In order to find the answers to all these questions, biologists, physicists and mathematicians have been studying smaller ecosystems and creating mathematical models to describe the dynamics of species, [3] [4] [5]. Although they are deterministic, these models can not be implemented with basic analytical tools given their large number of variables and dependencies, which requires employing methods of dynamical systems theory.

The bacteria *Escherichia coli*, abreviated as *E. coli*, are often chosen in experiments for their simplicity, fast growth, easy access and familiarity. These organisms were first discovered by Theodor Escherich, [6], in 1885, and nowadays hundreds of strains are known, [7]. They have a size of the order of 1 μm and can divide every 20 minutes , [8]. They are also found in the intestines of endotherms (commonly known as warm-blooded animals) and are able to grow in the presence of oxygen, which makes them easy and inexpensive to cultivate in a laboratory, [8].

In this thesis we show the modeling of populations consuming one or multiple types

of resources, reproducing and dying, using the law of mass action, [9], as well as with the Monod model, [3]. We also show the simulations resulting of these models and compare them to data obtained from our experiments or collected from other sources, [10], on *E. coli* growing in the presence of nutrients.

1.1 The first important growth models

The Malthusian and logistic models are still seen as the basis of many populational models today.

In 1798, the economist and demographer T. R. Malthus wrote a book on the population dynamics and in it described the first most important population growth model, [11]. Malthus stated that in the case where resources are unlimited, the population would grow indefinitely and its rate of growth would be proportional to the existing number of individuals of that population.

The Malthusian model can be deduced from the kinetic equations assuming that the number of individuals N of a population reproduce in the presence of a resource R, at a positive rate k (note that the resource is not wasted in the process)

$$R + N \xrightarrow{k} R + 2N\,. \tag{1.1}$$

Using the law of mass action, [12][9], the time equation describing the growth of the population N, in the presence of a constant resource R , can be obtained from the kinetic equations (1.1),

$$\begin{cases} \dfrac{dN}{dt} = k\,R\,N(t) \\ \dfrac{dR}{dt} = 0 \end{cases}. \tag{1.2}$$

The solutions of this system of equations are

$$\begin{cases} N(t) = N(0)\,e^{k\,R\,t} \\ R(t) = R(0) \end{cases}. \tag{1.3}$$

In this Malthusian model, resources are always available, which implies that the population will explode exponentially over time.

The mathematician P. F. Verhulst studied the census population numbers of the United States between 1790 and 1840, and in 1845 proposed a modification to the Malthusian model, where he included the consumption of resources, [13]. Opposed to

the model (1.1), the resource R is now expended as the reproduction happens,

$$R + N \xrightarrow{k} 2N. \tag{1.4}$$

The time equations for the population growth and resource consumption can be derived from equation (1.4) in the same way as before, using the mass action law, [9]:

$$\begin{cases} \dfrac{dN}{dt} = k\,R\,N \\ \dfrac{dR}{dt} = -k\,R\,N \end{cases}. \tag{1.5}$$

From the sum of these two equations we have

$$R(t) + N(t) = C = R(0) + N(0) \tag{1.6}$$

which is a conservation law defining the carrying capacity constant C, that prevents the population from growing perpetually.

The system (1.5) can be written in a different form

$$\begin{cases} \dfrac{dN}{dt} = k\,N\,(C - N) \\ \dfrac{dR}{dt} = -k\,R\,(C - R) \end{cases}, \tag{1.7}$$

which shows that these equations are logistic, and have the solutions

$$\begin{cases} N(t) = \dfrac{C\,e^{kCt}}{C/N(0) - 1 + e^{kCt}} \\ R(t) = \dfrac{CR(0)}{R(0) + [C - R(0)]e^{kCt}} \end{cases}. \tag{1.8}$$

From the first equation in (1.5), we get

$$\frac{1}{N}\frac{dN}{dt} = k\,R\,, \tag{1.9}$$

which is a linear relation between the normalized growth rate of the population and the amount of resources.

In 1969, the ecologist Robert MacArthur proposed the first mathematical consumer-resource model describing a group of B different species, each represented by the index β with N_β individuals, competing for J different types of common resources, each

represented by the index j, and introduced different timescales for the rates of supply and consumption, [14].

MacArthur assumed the rate of growth of a population, N'_β, to be proportional to the already existing population, N_β, the number of resources of each type, R_j, their relative importance measured by the weight parameter w_j, and the probability of an individual of that population to consume the different nutrients, $p_{\beta j}$. The number of resources of type j varies according to their current amount, the carrying capacity associated with the resource j, C_j, and to the probability of being eaten by any of the species and their population size. This model is assumed to be described by the logistic type equations

$$\begin{cases} \dfrac{N'_\beta}{N_\beta} = M_\beta\Big(\sum\limits_j p_{\beta j} w_j R_j - R_\beta^T\Big) \\ \dfrac{R'_j}{R_j} = r_j\Big(1 - \dfrac{R_j}{C_j}\Big) - \sum\limits_\beta p_{\beta j} N_\beta \end{cases} \tag{1.10}$$

where the ' represents time derivative. The constant R_β^T is the threshold mass of resource necessary to maintain the population, M_β is the proportion between the mass of resource and of the population it originates, and r_j is the maximum rate of resource variation. All these constants are non negative.

1.2 Observations and conceptual models

In 1934, the ecologist Georgy Gause enounced that in processes of competition for limited resources, one species would drive the others to extinction, [15] — the Gause's Law — based on observations of a culture with two species of single-celled eukaryotes (*Paramecium aurelia* and *Paramecium caudatum*) competing for the consumption of bacteria in an Osterhout's medium[1].

The Gause's Law was later reformulated by Garrett Hardin in 1960 and became known by the name Competitive Exclusion Principle, [16], stating that the number of species coexisting cannot exceed the number of resources. However, one year later, George Hutchinson noticed that *Plankton* could grow in situations of limited resources, [17], known as the Paradox of the Plankton, as we know today that happens in many other ecosystems, in violation of the Competitive Exclusion Principle. So a question arised: in what circumstances do competitive exclusion and sustainable coexistence take place?

[1] An Osterhout's medium is a salt solution composed by 104 mg of NaCl, 8.5 mg of $MgCl_2$, 4 mg of $MgSO_4$, 2.3 mg of KCl, and 1 mg of $CaCl_2$ per liter of water.

In 1941, Monod studied a culture of *E. coli* in a medium containing glucose and proposed a sigmoidal relation between the culture's normalized growth rate and its nutrient concentration R, [3]:

$$\frac{1}{N(t)}\frac{dN(t)}{dt} = g_{max}\frac{R(t)}{R_{1/2} + R(t)} \tag{1.11}$$

where $R_{1/2}$ is the concentration for which the growth is half the maximum, g_{max}.

Although revolutionary, this empirical model described a single species in the presence of a single nutrient which is too simplistic, since species depend on different nutrients for growth and are never isolated. Moreover it could only produce accurate results for short-term evolution.

Monod also discovered the diauxic growth. When bacteria are in the presence of different nutrients, they "evaluate" the energy cost of metabolizing each one *versus* the growth rate they will provide (how valuable the resource is), and choose the preferred nutrient. In this way, bacteria consume the nutrients sequentially by order of the most to the least favorable, generating different growth rate phases over time, named diauxies. This adaptative mechanism ensures an optimization strategy: it allows the species to have the biggest growth rate when the population is small (and thus, more fragile) and provides a smaller growth rate when the population becomes bigger (and the risk of extinction is smaller).

> "*Diauxie — This phenomenon is characterized by a double growth cycle consisting of two exponential phases separated by a phase during which the growth rate passes through a minimum even becoming negative in some cases.*"
>
> —$Monod$

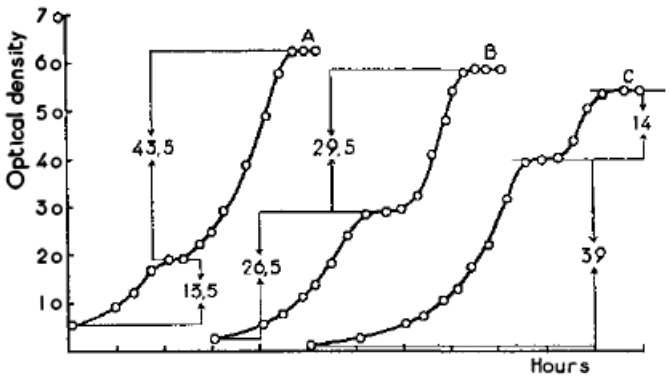

Figure 1.1: *E. coli* density over time in a medium composed by glucose and sorbitol in different proportions: A: Glucose 50 µg/ml; sorbitol 150 µg/ml. B: Glucose 100 µg/ml; sorbitol 100 µg/ml. C: Glucose 150 µg/ml; sorbitol 50 µg/ml. Adapted from [3].

Figure 1.1 shows the result of an experiment done by Monod in which he studied the growth of a culture of *E. coli* in a medium with two nutrients – Glucose ($C_6H_{12}O_6$) and Sorbitol ($C_6H_{14}O_6$). When varying the concentrations of each nutrient, the growth phases are proportional to the nutrient concentrations, showing that bacteria consumed the nutrients separately by order.

However, Monod's growth model (1.11) could not explain the diauxic growth he observed.

Inspired by previous works of MacArthur and Edward Wilson, [18] [19], in 2001, the ecologist Stephen Hubbell examined the biodiversity in ecological communities looking at the abundance distribution of species in different locations (fig. 1.2).

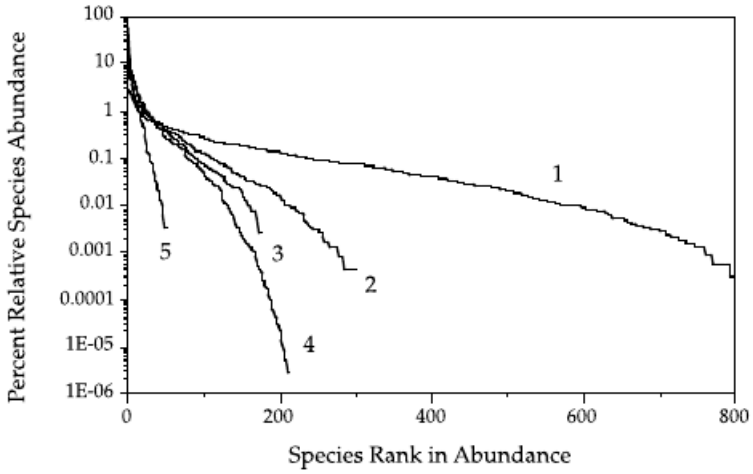

Figure 1.2: Relative population sizes of 5 ecological communities ranked from the largest to the smallest. 1: Tropical wet forest in Amazonia. 2: Tropical dry deciduous forest in Costa Rica. 3: Marine planktonic copepod community from the North Pacific gyre. 4: Terrestrical breeding birds of Britian. 5: Tropical bat community from Panama. Adapted from [20].

Hubbell noticed that the curves had similar shapes, which lead him to wonder if there would exist a theory behind it and, if so, whether the curves were possible to predict. To explain this pattern, he created the Unified Neutral Theory of Biodiversity [20] in which species were grouped by ecological communities. The theory stated that species that occupied the same geographic area and level in a food chain were seen as equally strong. In a neutral setup, the individuals were considered identical in terms of average probabilities of birth, death, migration and speciation. Only small random deviations in this quantities were responsible for changes in population which meant that biodiversity arised from stochastic processes, that is, random fluctuations of external variables.

In 2010, Matthew Scott, Carl Gunderson, Eduard Mateescu, Zhongge Zhang and

Terence Hwa designed and conducted a series of experiments which showed that the growth rate of *E. coli* is proportional to the ratio between the cells RNA and protein [21].

In 2014, Guillaume Lambert and Edo Kussell did a series of experiments with cultures of *E. coli* feeding off glucose and lactose alternately [22]. They noticed that when consuming the same nutrient as before, the lag phases of the transitions between nutrients shortened, even if the daughter cells had never consumed the nutrients. They concluded that this phenomenon was associated with a non-genetic memory. Four years later, Cerelus et al., [23], discovered different molecular mechanisms related to this history-dependent behavior and observed that the duration of the lag phase was proportional to the amount of time the cells were feeding off the other nutrient.

1.3 Recent models

Based on the MacArthur's model (1.10), Posfai, Taillefumier and Wingreen presented a resource-competition model in 2016, [4], that accounted for the fact that organisms work with a limited amount of energy and therefore, need to choose how to allocate different fractions in order to favor the traits that maximize the species' probability of survival. This sometimes means reducing certain performances in order to enhance others (trade-offs). This model predicted that coexistence of species could occur in cases where, according to the Competitive Exclusion Principle, could not, reproducing what happens in many ecosystems, [17].

Similarly to the MacArthur' model, the population growth rates (N'_β) vary according to the current number of individuals (N_β) of each population (β), the death rates (δ_β), the nutritional values (v_j) and nutrients availability (A_j), and the consumption rates ($\alpha_{\beta j}$) of every resource j by each species β, called "metabolic strategies". The variations of resources concentrations (R'_j) are proportional to their supply rates (s_j) and decrease with the rates of consumption ($\alpha_{\beta j}$) and degradation (d_j):

$$\begin{cases} N'_\beta = N_\beta \left[\sum_{j=1}^{J} v_j \alpha_{\beta j} A_j(R_j) - \delta_\beta \right] \\ R'_j = s_j - \sum_{\beta=1}^{B} N_\beta \alpha_{\beta j} A_j(R_j) - d_j R_j \end{cases}, \tag{1.12}$$

where

$$A_j(R_j) = \frac{R_j}{K_j + R_j} \tag{1.13}$$

is a Monod type of function with K_j being the concentration for which A_j is half the

maximum. The metabolic strategies are constrained by the maximum uptake rate U_β they are capable of,

$$\sum_{j=1}^{J} w_j \alpha_{\beta j} = U_\beta. \tag{1.14}$$

Posfai et al. tested the possibility of coexistence of a system consisting of three species in the presence of three nutrients with different supply rates. In this case, by equation (1.14), given two metabolic strategies for a certain species, the third one is automatically determined. Thus, a triangular plot, where the axes go from 0 to 1, i.e., a simplex plot, is the perfect way to visualize the distribution of metabolic strategies.

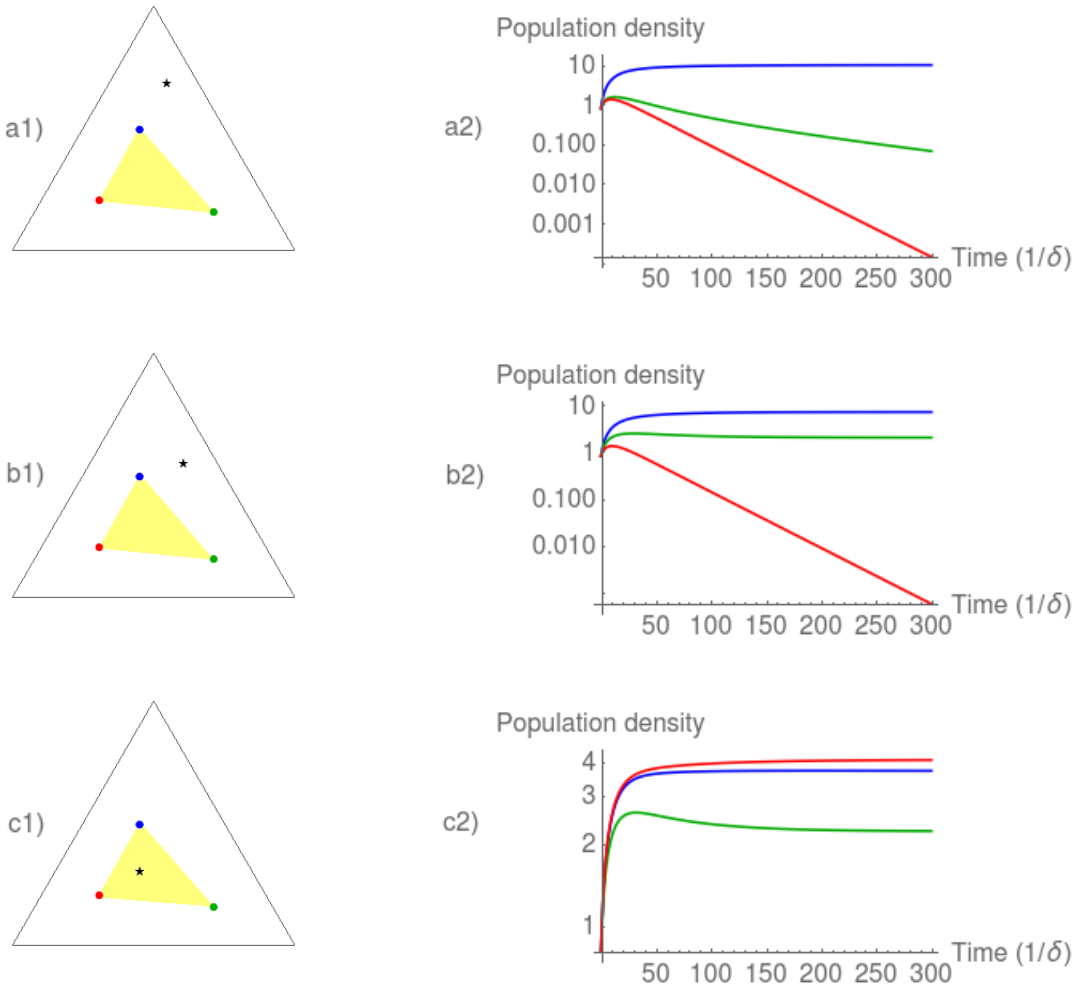

Figure 1.3: Left: simplex plots with metabolic strategies of 3 species ($B = 3$) relative to 3 different resources ($J = 3$) represented by colored dots: $\alpha_{1j} = (0.30, 0.20, 0.50)$ in blue, $\alpha_{2j} = (0.20, 0.65, 0.15)$ in green, $\alpha_{3j} = (0.60, 0.20, 0.20)$ in red, the convex-hull of metabolic strategies in yellow triangles, and the supply rates a1) $s = (0.10, 0.20, 0.70)$, b1) $s = (0.10, 0.35, 0.55)$ and c1) $s = (0.40, 0.30, 0.30)$ in black stars. Right: simulations obtained with model equations (1.12), (1.13) and (1.14) for the evolution of the 3 population densities, $N_\beta(t)/N_\beta(0)$, with parameters $d = 0.1$, $\delta = 0.1$, $R = 1$, $v = 1$, $K = 1$, $w = 1$, $U_\beta = 1$ and the chosen constants for the corresponding simplexes, for times between 0 and $300/\delta$. Note that we have taken the same parameters for all three species.

Figure 1.3 shows our simulations reproducing the Posfai et al. work. The three simplex plots contain the initial metabolic strategies of each species, represented by dots, and the nutrients' supply rates, by a star. Next to it, are the respective evolutions of the population densities, $N_\beta(t)/N_\beta(0)$, over time.

The results indicate, from top to bottom, that as the supply rates fall into the area delimited by the metabolic strategies — the convex-hull — the coexistence becomes possible. This, of course, discloses the importance of having certain species in an ecosystem. The addition of a species whose metabolic strategies allow to enclose the

supply rates is determinant to the future of all the other species.

In the first system of figure 1.4, composed by 14 species, it can be seen that most go to extinction. However, if a new determinant species is inserted in the system, this no longer happens and all species can coexist.

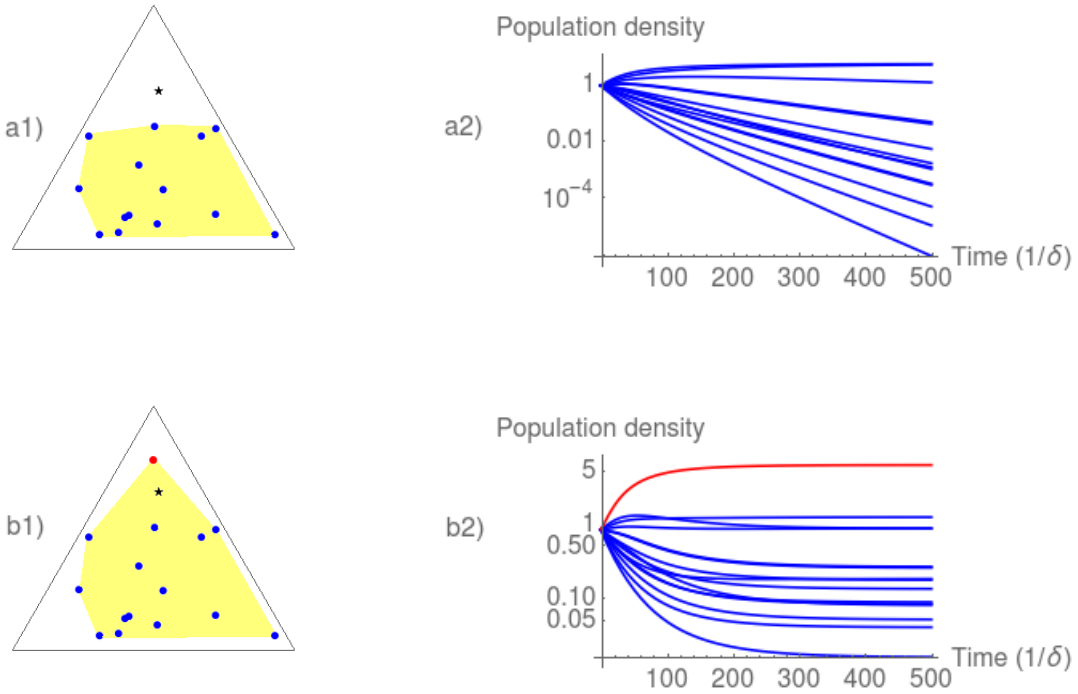

Figure 1.4: Left: simplex plots with metabolic strategies of 15 species ($B = 15$) relative to 3 different resources ($J = 3$) represented by blue (14) and red (1) dots, convex-hull of metabolic strategies in yellow polygons, and supply rates $s = (0.15, 0.19, 0.66)$ in a black star. The metabolic strategies in blue were chosen randomly between 0 and 1 such that their convex-hull would not include the supply rates. The metabolic strategies in red were chosen such that the new convex-hull formed by the 15 species would include the supply rates. Right: simulations obtained with model equations (1.12) for the evolution of the same 14 and 15 population densities, $N_\beta(t)/N_\beta(0)$, with parameters $d = 0.1$, $\delta = 0.1$, $R = 1$, $v = 1$, $K = 1$, $w = 1$, $U_\sigma = 1$ for times between 0 and $500/\delta$.

Motivated by the Unified Neutral Theory of Biodiversity of Hubbell, [20], Posfai et al. decided to incorporate demographic stochasticity in their model.

They assumed that the growth rate (N'_β) of the population of the species β is proportional to its existing population (N_β), amount of resources (R_j) of each type (j), their consumption by the species β, and death rates (δ_β). The consumption rates consist in a constant metabolic strategy ($\alpha_{\beta i}$) and a random variable ($\xi_{\beta j}$) with Gaussian distribution $\mathcal{N}(0, \sigma^2)$. Similarly, the death rates (δ_β) are given by the sum of a constant, 1, and the random variable (ξ_β) with the same distribution. The amount of resource (R_j) of each type (j) are proportional to their supply rates (s_j) and inversely proportional to the rates of consumption and number of individuals (N_β).

$$\begin{cases} N'_\beta = \left[\sum_{j=1}^{J} \left(\alpha_{\beta j} + \xi_{\beta j} \right) R_j - \delta_\beta \right] N_\beta \\ R_j = \dfrac{s_j}{\sum_{\beta=1}^{B} N_\beta \left(\alpha_{\beta j} + \xi_{\beta i} \right)} \\ \delta_\beta = 1 + \xi_\beta \end{cases} \tag{1.15}$$

The metabolic strategies ($\alpha_{\beta j}$) and supply rates (s_j) are normalized such that

$$\sum_{j=1}^{J} \alpha_{\beta j} = 1 \quad \text{and} \quad \sum_{j=1}^{J} s_j = \sum_{\beta=1}^{B} N_\beta(0). \tag{1.16}$$

Implementing the previous model they obtained the results shown in figure 1.5. The model was able to reproduce the curves identified by Hubbell.

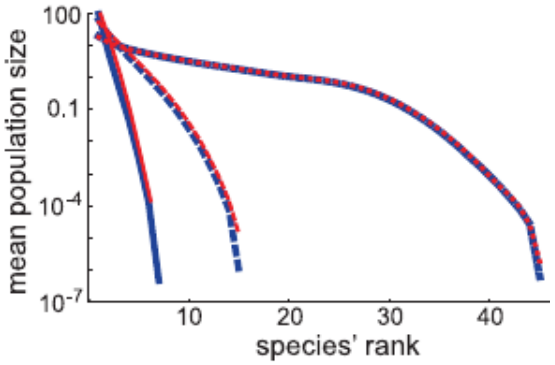

Figure 1.5: Simulation of rank-abundance curves obtained with model equations (1.15) and (1.16) for a total population of 100 individuals competing for 3 resources equally supplied. The solid, dashed and dotted curves correspond to immigration probabilities of 0.001, 0.01 and 0.1 respectively. Adapted from [4].

In December 2018, Pacciani-Mori, Suweis and Maritan constructed a model that assumed the same equations as Posfai et al., (1.12), (1.13) and (1.14), but dynamic

metabolic strategies instead of fixed ones, [5]. Doing so, they introduced the fact that species have the ability to adapt to changes in the environment by regulating gene expression, in this case, nutrients' concentrations (R_j). To achieve that, Pacciani-Mori et al. required species to adapt in a favorable way, i.e., so that they would evolve in order to maximize their growth rate:

$$\alpha'_{\beta j} \propto \frac{\partial}{\partial \alpha_{\beta j}} \left(\sum_{j=1}^{J} v_j \alpha_{\beta j} A_j - \delta_\beta \right). \tag{1.17}$$

Since δ_β is the death rate of species β, $1/\delta_\beta$ is a natural choice for the characteristic time scale of the evolution of population β. Therefore, the characteristic time scale of evolution of the metabolic strategies can be written as a multiple of $1/\delta_\beta$, given by a parameter ρ.

Now that the metabolic strategies are dynamic, there is a maximum uptake rate (U^*_β) for each species: $\sum_j w_j \alpha_{\beta j}(t) = U_\beta(t) \leq U^*_\beta$. Similarly, the nutrient uptake rates U^*_β can be written as $Q\delta_\beta$. Therefore, the evolution of metabolic strategies is described by the equation

$$\alpha'_{\beta j} = \alpha_{\beta j}\, \rho\, \delta_\beta \left[v_j A_j - \Theta \left(\sum_{j=1}^{J} w_j \alpha_{\beta j} - Q\delta_\beta \right) \frac{w_j}{\sum_{k=1}^{J} w_k^2 \alpha_{\beta k}} \sum_{l=1}^{J} v_l A_l w_l \alpha_{\beta l} \right]. \tag{1.18}$$

The full calculation of equation (1.18) is rather lengthy and can be found on page 4 of the supplemental material of [5]. The Heaviside-theta function prevents the metabolic strategies from taking negative values.

Pacciani-Mori et al. tested the model of equations (1.12), (1.13) and (1.14) with the addition of equation (1.18), for the growth of one species only in the presence of two different nutrients in order to reproduce the observations of Monod. The results are shown in figure 1.6.

The individuals consume the first resource until it ends at $t \approx 0.11$, [see figure 1.6b) in orange]. When this happens, the metabolic strategy corresponding to this resource changes, [see figure 1.6c) in orange], and the population suffers a diauxic shift, [see figure 1.6a)]. Then, the individuals consume the second resource until it ends at $t \approx 0.30$ [see figure 1.6b) in blue]. When this happens, the metabolic strategy corresponding to this resource changes [see figure 1.6c) in blue] and the population starts having a negative growth [see figure 1.6a)].

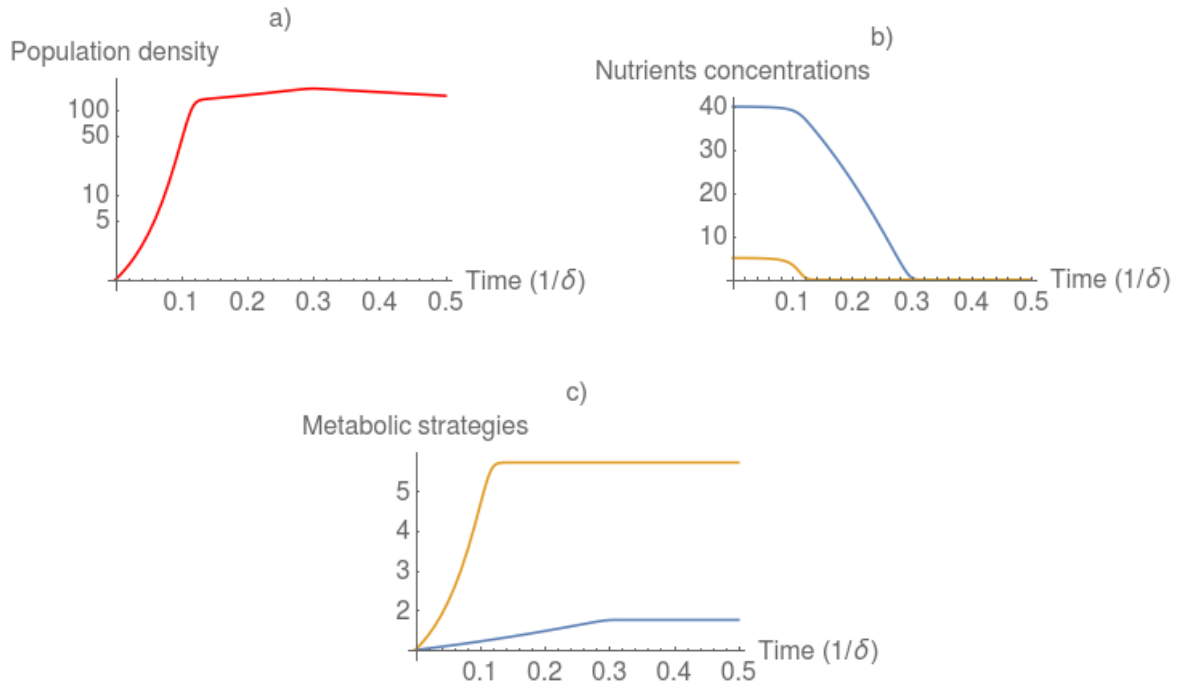

Figure 1.6: Simulations obtained with model equations (1.12), (1.13), (1.14) and (1.18) for 1 population of individuals of the same species with access to 2 resources of different properties. Results of the simulation for a) the population density, b) nutrient concentrations and c) respective metabolic strategies, with parameters $\vec{v} = (2, 25)$, $\vec{w} = (1, 4)$, $\vec{K} = (1, 3)$, $Q = 25$, $\delta = 1$ and ρ for times between 0 and $500/\delta$.

We've already seen that with the model constructed by Posfai et al., when the supply rates fall outside of the convex-hull of metabolic strategies, the coexistence of the initial set of species becomes impossible. However, they did not consider the adaptability of species. Pacciani-Mori et al. repeated the same simulations as Posfai et al. did, adding this detail and compared the results.

Figure 1.7 shows the results of the simulations obtained with model equations (1.12), (1.13), (1.14) and (1.18). Observing the simplex plot, it is possible to understand that, over time, the metabolic strategies evolved in a way such that their convex-hull would include the supply rates. By doing this, species become more fit to survive, as the consumption rates of each resource become compatible with their supply rates. Analyzing the plots that display this evolution, fig. 1.7 c1) and c2), we can identify that adaptation period ($0 < t \lesssim 100$) following by the stabilization of the populations and metabolic strategies ($t \gtrsim 100$), in contrary of what is obtained in the fixed metabolic strategies model of Posfai et al., figure 1.7 b). These results exhibit that adaptation is crucial to the survival of species when in a sub-ideal initial setting.

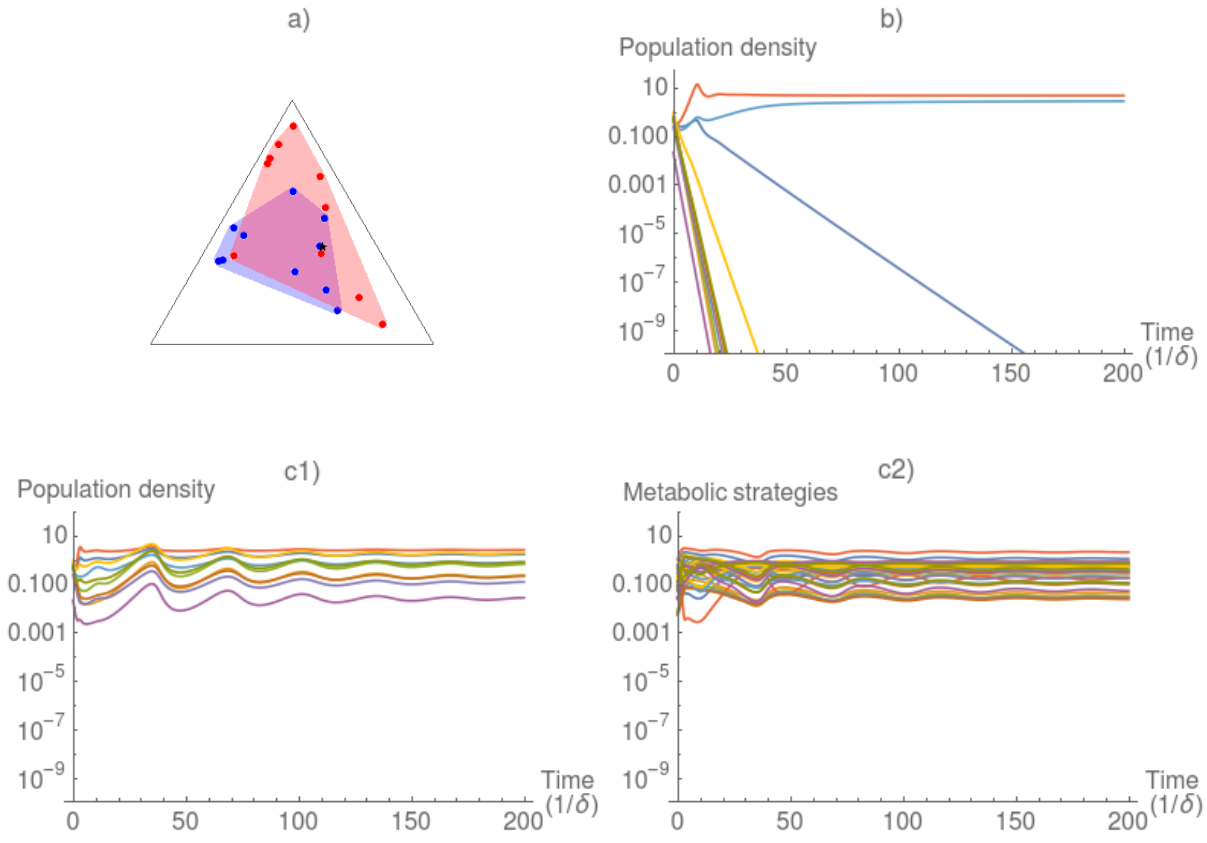

Figure 1.7: Simulation obtained with model equations (1.12), (1.13), (1.14) and (1.18) for the evolution of 10 population densities ($B = 10$) competing for 3 different resources ($J = 3$) during 200 time steps. a) simplex plot with initial and final metabolic strategies (and respective convex-hulls) represented in blue and red respectively and supply rates in a black star; b) evolution of the population densities in the case where the metabolic strategies are fixed; c1) evolution of the population densities in the case where the metabolic strategies are adaptative; c2) evolution of the metabolic strategies in the adaptative case; The parameters used were $Q = 2$, $d = 0$, $\delta_\beta \in \mathcal{U}[1, 1.5]$ ($\mathcal{U}$ being the uniform distribution), $U_\sigma \in \mathcal{U}[0, Q\delta_\sigma]$, $v_j \in \mathcal{U}[1, 2]$, $w_j \in \mathcal{U}[0, v_j Q]$, $N_\beta(0) \in \mathcal{U}[0, 1]$, $R_j(0) \in \mathcal{U}[0, 1]$, $K_j \in \mathcal{U}[1, 5]$, $s_j \in \mathcal{U}[0, 5]$, $\alpha_{\beta j}(0) : \sum_j w_j \alpha_{\beta j}(0) = U_\beta(0)$.

Of course, as species have a certain dynamic, so do their surroundings. In nature, resources are subject to large fluctuations over time, with many factors, for example the seasons. Pacciani-Mori et al. tested the robustness of an ecosystem subject to these fluctuations and the importance of having adaptative mechanisms to react to them. They considered variable supply rates with some periodicity where their values would lie inside the convex-hull of metabolic strategies (s_{in}) for a time τ_{in} and then change to another outside (s_{out}) for a time τ_{out}.

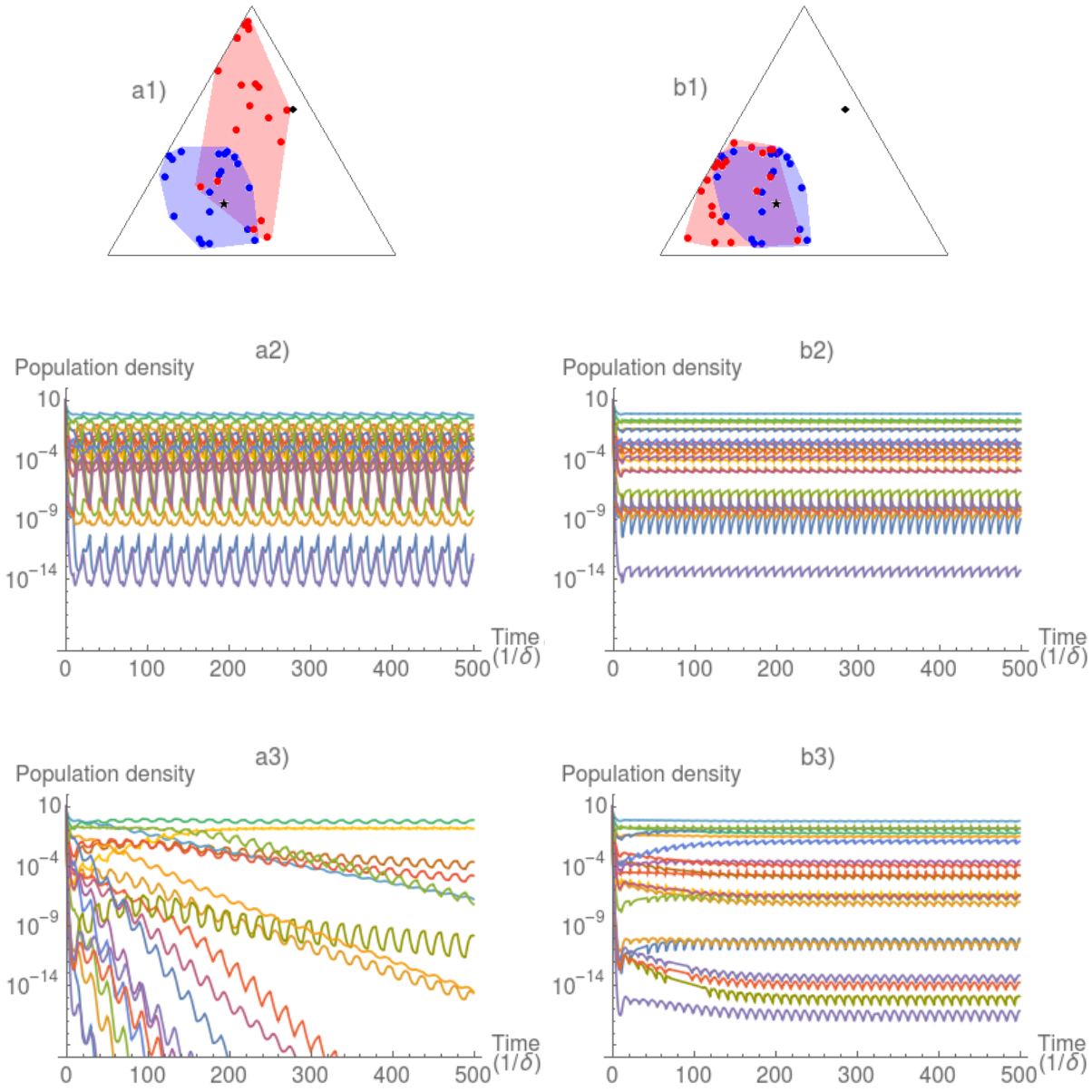

Figure 1.8: Simulation obtained with model equations (1.12), (1.13), (1.14) and (1.18) for the evolution of 20 population densities ($B = 20$) competing for 3 different resources ($J = 3$) during 500 time steps. $Q = 2$, $d = 0$; a1) Simplex plot with initial and final metabolic strategies (and respective convex-hulls) represented in blue and red respectively for $\tau_{in} = \tau_{out} = 10$; In a black star and diamond are represented respectively the supply rates that lie inside and outside the convex-hull of metabolic strategies; b1) same as previous but with $\tau_{in} = 10$ and $\tau_{out} = 1$; a2) adaptative metabolic strategies, $\tau_{in} = \tau_{out} = 10$; a3) fixed metabolic strategies, $\tau_{in} = \tau_{out} = 10$; b2) adaptative metabolic strategies, $\tau_{in} = 10$ and $\tau_{out} = 1$; b3) fixed metabolic strategies, $\tau_{in} = 10$ and $\tau_{out} = 1$.

In the cases where the species had the ability to adapt to the fluctuations of nutrient supplies, using equation (1.18), we can see that they all survived, fig. 1.8 a2) and b2), only varying the population with the same periodicity as the supply rates did.

However, when removing the adaptation system, by fixing the metabolic strategies in time, this behavior changes, fig. 1.8 b1). If the supply rates lie outside the convex-hull of metabolic strategies for too long, the coexistence becomes compromised, fig. 1.8 b1). Species can only coexist as long as the time outside the convex-hull, τ_{out} is small compared to τ_{in}, fig. 1.8 b3). We can also observe that the metabolic strategies evolve in a way that they include the supply rates s_{out} when they spend enough time outside the convex-hull, fig. 1.8 a1), thus violating the Competitive Exclusion Principle, and that it does not happen when that time interval is small, fig. 1.8 a3), impeding sustainable coexistence.

The populational models developed until now allow us to describe the growth rate of populations in terms of parameters but they lack an explanation for what mechanisms originate variations on the rate of growth. Also, they do not take into account the necessity of more than one nutrient for growth or explain the process of cells developing the metabolic strategies.

Chapter 2

Another approach to populational biology

As we have seen before, the models in use for the study of bacterial growth are empirical, i.e. without biological foundations. Because of this, we decided to focus on creating a model based on the known and measurable biological mechanisms of reproduction.

There are two alternative constructions: the more traditional, where the species-resource, species-species and species-genetics interactions are included, and the phenomenological, successfully used in Tetrahymena, [24], mouse, and human populations, [25]. This model was develop by the epidemiologist Anderson McKendrick (also known as the McKendrick-von Foerster equation). Nevertheless, the produced results should be the same regardless of the modeling techniques.

We start with a phenomenological model in which the reproduction is only controlled by a time interval with a memory effect, in section 2.2, leading to the Malthusian function. In section 2.3 we add nutrient consumption with stochastic fluctuations to the model, and the reproduction is controlled by the synthesized protein. The resulting microscopical function is sigmoidal, as in the Verhulst case. To backup our models, we prepared a series of experiments, shown in section 2.4, which were carried out at the Instituto Gulbenkian de Ciência, and then analyzed the results using *Mathematica*'s integrated functions, developed feedback fitting methods and statistics tools. We also analyze existing data from another experiment, [10], in section 2.5.

In section 2.6 we develop a model in which reproduction and death are controlled by species-resource interactions. From this model, there arises the toxicity effect explained by Lambert and Cerelus, [22] [23], not present in the previous models. Section 2.7 contains a generalization of the previous model including two nutrients. The model presents a toxicity effect and diauxies. To test the models of sections 2.6 and 2.7 we design an experiment plan, shown in section 2.8.

2.1 Statistical analysis and Fitting methods

Note: All the indices and variables used in this section are arbitrary and have no correlation to the rest of the variables used in other sections.

Let E be a set containing some experimental data, T the set of corresponding theoretical points, and N the number of data points, i.e. the cardinality of those sets. We can consider two vectors with components E_i and T_i ($0 < i \leq N$) constructed from the sets. Then,

1) the Pearson's chi-squared [27],

$$\chi^2 = \sum_{i=1}^{N} \frac{(E_i - T_i)^2}{T_i} \tag{2.1}$$

is a normalized quantity between 0 and ∞, geometrically interpreted as the radius of a $(N-1)$–dimensional ellipse composed of the N normalized deviations obtained from the pairs of the two vectors, that indicates how close (the radius) the analogous components of the two vectors are.

2) the Pearson's correlation coefficient [26] is a quantity between -1 and 1 that measures the linear correlation between the pairs of the vectors, 1 being the total correlation between the two (E and T follow the same growth), 0 no correlation, and -1 total inverse correlation. It is defined by the following mathematical function

$$\rho(E,T) = \frac{\mathrm{cov}(E,T)}{\sigma_E\, \sigma_T} \tag{2.2}$$

in which the co-variance $\mathrm{cov}(E,T)$ is given by

$$\mathrm{cov}(E,T) = \frac{1}{N-1} \sum_{i=1}^{N} (E_i - \bar{E})(T_i - \bar{T}), \tag{2.3}$$

and the standard deviation σ_X and mean value $\bar{X}$ of a variable X are given by

$$\sigma_X = \sqrt{\frac{1}{N-1} \sum_{i=1}^{N} (X_i - \bar{X})^2}, \quad \bar{X} = \frac{1}{N} \sum_{i=1}^{N} X_i\,. \tag{2.4}$$

Inserting the definitions (2.3) and (2.4) in (2.2) we obtain

$$\rho(E,T) = \frac{(N-1)^{-1}\sum_{i=1}^{N}(E_i-\bar{E})(T_i-\bar{T})}{\sqrt{(N-1)^{-1}\sum_{i=1}^{N}(E_i-\bar{E})^2}\sqrt{(N-1)^{-1}\sum_{i=1}^{N}(T_i-\bar{T})^2}} \tag{2.5}$$

$$= \frac{\sum_{i=1}^{N}(E_i-\bar{E})(T_i-\bar{T})}{\sqrt{\sum_{i=1}^{N}(E_i-\bar{E})^2}\sqrt{\sum_{i=1}^{N}(T_i-\bar{T})^2}}$$

3) the Spearman's rank correlation coefficient [28]

$$\rho_r(E,T) = \frac{\sum_{i=1}^{N}(r_{E_i}-\overline{r_E})(r_{T_i}-\overline{r_T})}{\sqrt{\sum_{i=1}^{N}(r_{E_i}-\overline{r_E})^2}\sqrt{\sum_{i=1}^{N}(r_{T_i}-\overline{r_T})^2}} \tag{2.6}$$

in which r_{X_i} is the ranking of the element X_i in the set X, has the same mathematical form as the Pearson correlation coefficient. However, it focuses on the ranking of the variables, i.e., it responds to the similarities of the monotonic tendencies of the data.

Mathematical models to fit data and test the goodness of a fit:

- The `FindFit` function of the software *Mathematica* is a statistical test used to fit non linear models. It defines the sum of the squares of the residuals, s, in terms of the fitting parameters a_k, in which k is the number of parameters, and solves the partial differential equations (2.7) to find the values of a_k that give the minimum of s,

$$\partial_{a_k} s = 0. \tag{2.7}$$

- In the method of random variables developed by us, we attribute random values to the set of variables we want to fit. We start by finding the range of the orders of magnitude of those variables, by plotting the data and the function for fit, using the `Manipulate` function of *Mathematica*. This allows us to search visually for that range. Then we design a loop where in each iteration, the variables take a random value within the ranges we found, and use one of the statistic analysis methods above (we use the Pearson's χ^2 and the Spearman's correlation) to test how appropriate the values are, that is the goodness of fit of the function to the data.

2.2 First model: Mitosis with memory

The first model we consider is overly simplistic, consisting in a single population of cells in the presence of an inexhaustible nutrient supply. However, in general, mitosis time, i.e., the time cells take to divide into two, depends on the pressure, temperature and availability of resources in a complex manner and for that reason we opted by a stochastic model.

We assume that, initially, every cell (i) from the population divides itself after 3 hours, the first generation time (τ_{1i}). All cells are considered to have memory, such that the generation time of the daughter cells (τ_{2i}) will be given by

$$\tau_{\gamma i} = \tau_{\gamma-1,\lceil \frac{i}{2} \rceil} + \epsilon \tag{2.8}$$

in which ϵ is a random variable obeying the normal distribution centered at zero and with some standard deviation σ, i.e. $\mathcal{N}(0, \sigma^2)$.

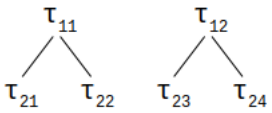

Figure 2.1: Scheme of generation times from the reproduction of two bacteria in the first generation and giving birth to 4 bacteria of the second generation.

In figure 2.2 we show the result of the simulation of a population over 40 hours, obtained using the model equation (2.8), starting with a single cell. As a result of ϵ, the mitosis lose their initial synchronization gradually and produce a macroscopic trend curve consistent with the Malthusian model, as observed by the biologist D. M. Prescott in 1959, [30] (see figure 2.3). The distribution of the mitosis ages is Gaussian, as expected since the desynchronization comes from the the stochasticity of the variable ϵ. Rubinow [24] arrived to the same distributions using the experimental data from the work of Prescott [30].

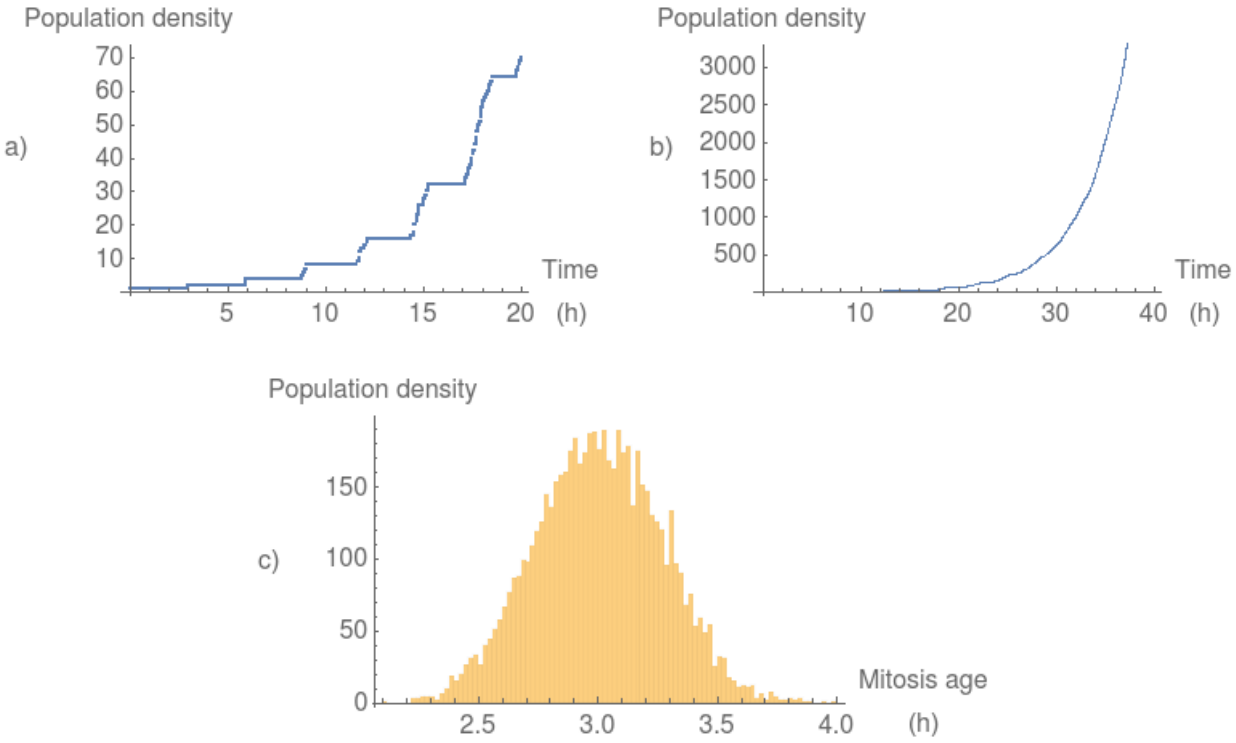

Figure 2.2: a) Growth curve of a population for 20 hours starting with 1 cell with mitosis time of 3h; ϵ is randomly chosen from a normal distribution with mean value 0.0 and standard deviation 0.1; b) Growth curve of a population for 40 hours with the same conditions as in a); c) distribution of all the ages of mitosis occurred during the 40 hours population growth.

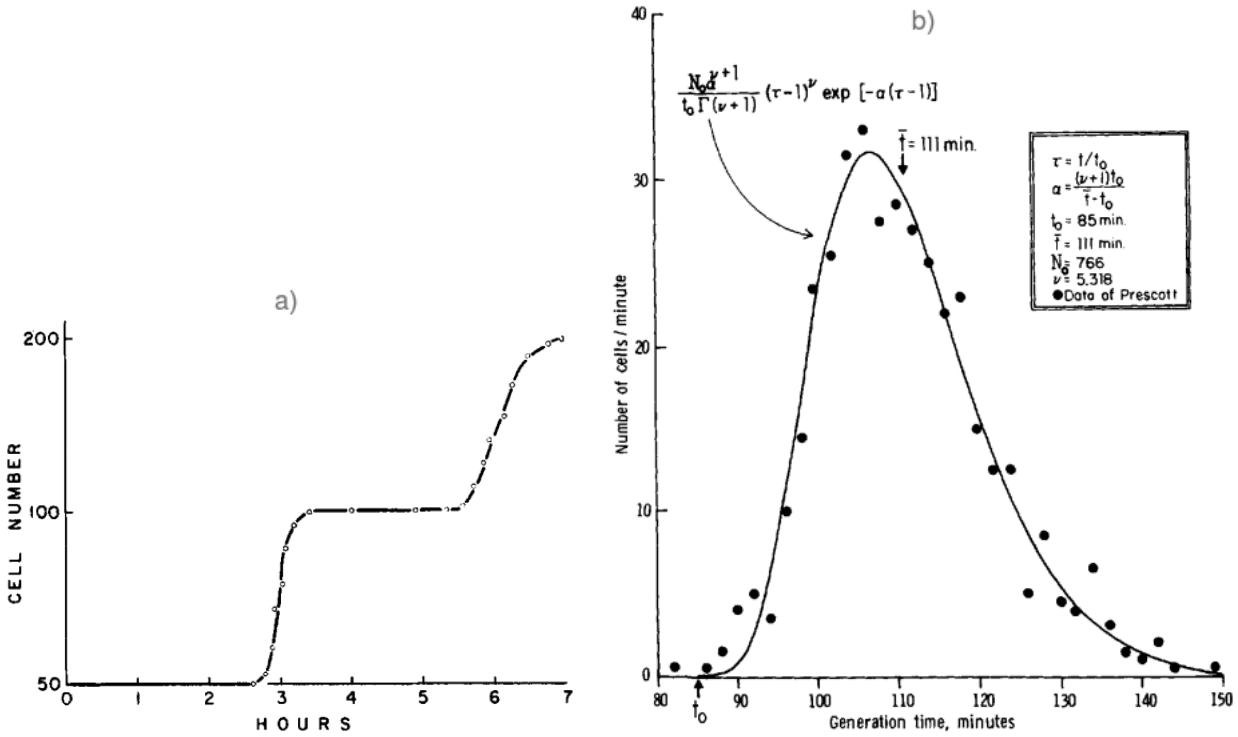

Figure 2.3: a) Growth curve of a population of *Tetrahymena pyriformis* over two generations, with mitosis moments initially synchronized, [30]. b) Distribution of the mitosis ages taken from the data in a), [24].

By doing a fit of the simulation the population density, N, over time for the case where $\epsilon = 0$, we discover that the curve a is power function (see figure 2.4) of the form $N \approx 1.213^t$ (figure 2.5) in agreement with [9].

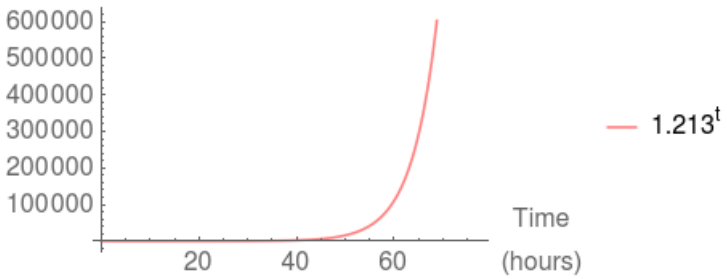

Figure 2.4: Power function $f(t) = 1.213^t$

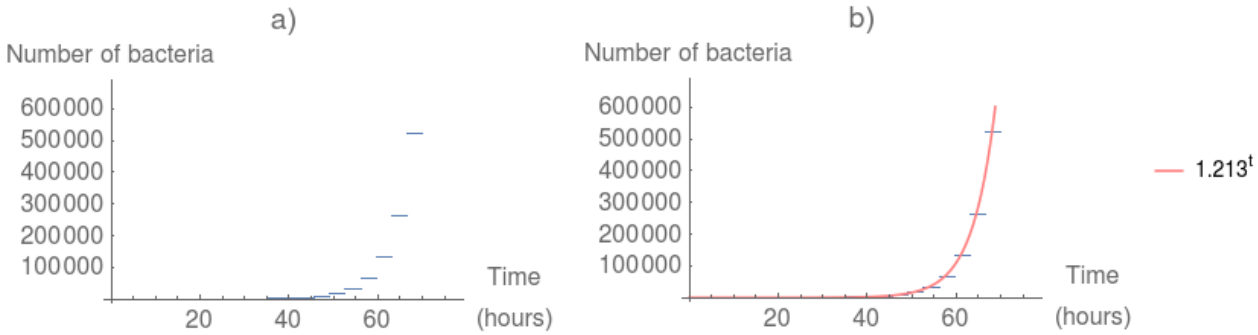

Figure 2.5: a) Growth curve of a population for 65 hours starting with 1 cell and all mitosis times of 3.5 hours; b) The fit of the data gives $N \approx 1.213^t$ — fit executed with the `FindFit` function of the software *Mathematica* and validated by the Spearsman's rank coefficient $\rho_r = 0.999$.

2.3 Second model: Mitosis controlled by the consumption of a single nutrient

In the second model, we assume that the nutrients available are limited. In reality, cells uptake the nutrient from the medium and then use it to produce essential proteins and energy, a process called metabolization. Once the cell has metabolized enough resources, a threshold P^*, it begins mitosis, [30].

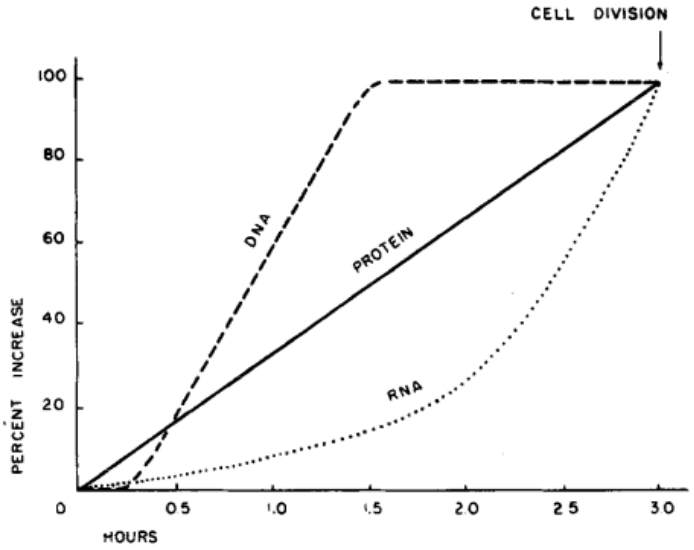

Figure 2.6: Image taken from Prescott, [30], illustrating the process necessary for the reproduction of a cell.

Consider that we have an initial number of cells $N(0)$ in a medium where there is a starting amount of nutrient $R(0)$. We assume that the probability of a cell, i, finding a nutrient is proportional to the quantity of existing nutrient at that time t, $R(t)$, and the duration of the search, Δt. Also, we consider that the uptake of nutrients in a true environment is subject to stochastic fluctuations, for which we add the parameter λ, randomly chosen from the distribution $\mathcal{N}(1.5 \times 10^{-4}, 2 \times 10^{-4})$ in each time step.

Therefore, during a time interval Δt, the cell i metabolized protein $P_i(\Delta t)$ is given by $\lambda_i R(t)\Delta t$ and thus, the total amount of protein produced at an instant can be written as a recursion relation:

$$P_i(t + \Delta t) = P_i(t) + \lambda_i R(t)\Delta t, \tag{2.9}$$

that can be rearranged as

$$\frac{P_i(t + \Delta t) - P_i(t)}{\Delta t} = \lambda_i R(t). \tag{2.10}$$

Taking the previous equation in the limit $t \to 0$ we obtain

$$\frac{dP_i}{dt} = \lambda_i R(t). \tag{2.11}$$

In the same way, the amount of nutrient still available at an instant $t + \Delta t$ is equal to the amount of nutrient there was in the previous moment minus the amount of nutrient

that was consumed by all the cells in that time interval,

$$R(t+\Delta t) = R(t) - \sum_{i=1}^{N} \lambda_i R(t)\Delta t, \tag{2.12}$$

that can be rearranged as

$$\frac{R(t+\Delta t) - R(t)}{\Delta t} = -\sum_{i=1}^{N} \lambda_i R(t). \tag{2.13}$$

Taking the previous equation in the limit $t \to 0$ we obtain

$$\frac{dR}{dt} = -\sum_{i=1}^{N} \lambda_i R(t). \tag{2.14}$$

We implemented the model equations (2.9) and (2.12) to simulate the growth of a population starting with one cell during 168 hours and found a sigmoidal function that best fitted the curve (a simplified program code is presented in appendix A2). Figure 2.7 shows the resultant growth curve and fit.

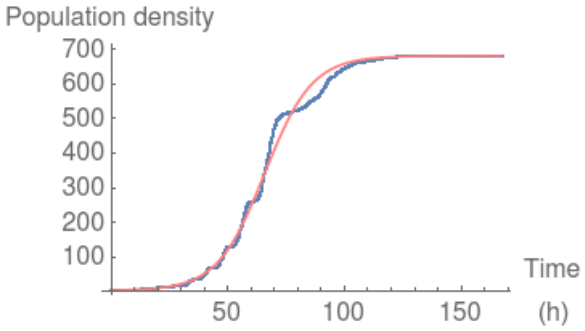

Figure 2.7: In blue: simulation obtained with model equations (2.9) and (2.12) for the evolution of a population starting with 1 cell, feeding off 1 nutrient and with threshold protein $P^* = 1$ during 168 hours. The parameter λ varied according to the normal distribution with parameters $\mu = 1.5 \times 10^{-4}$ and $\sigma = 2 \times 10^{-4}$) truncated between 0 and 2μ and normalized; In red: the correspondent logistic function 1.8 with parameters $c = 679$ and $k \approx 0.0003$ obtained with the `FindFit` function of the software *Mathematica*, corresponding to a Spearsman' rank coefficient $\rho_r = 0.927$.

To study the influence of the stochasticity in the evolutions of the population and nutrient, we tested different distributions for the parameter λ (see figures 2.8 and 2.9).

Observing figure 2.8 from top to bottom we can see that when the mean value, μ, increases, the bacteria eat in average more resources in each time step, so the population curve shifts left and becomes steeper, which translates to a faster growth that starts sooner. The histogram of the mitosis ages takes the same shape, but be-

comes less scattered, since the bacteria take less time to reach the protein threshold necessary for reproducing.

In figure 2.9 when the standard deviation σ increases, the desynchronization increases, i.e., the population curve becomes smoother, and macroscopically it takes a logistic shape; The histograms become more scattered since the nutrient uptakes are also more disparate.

Plotting the relation between the normalized growth rate and nutrient obtained from the same simulated data, we discover a linear curve, shown in figure 2.10.

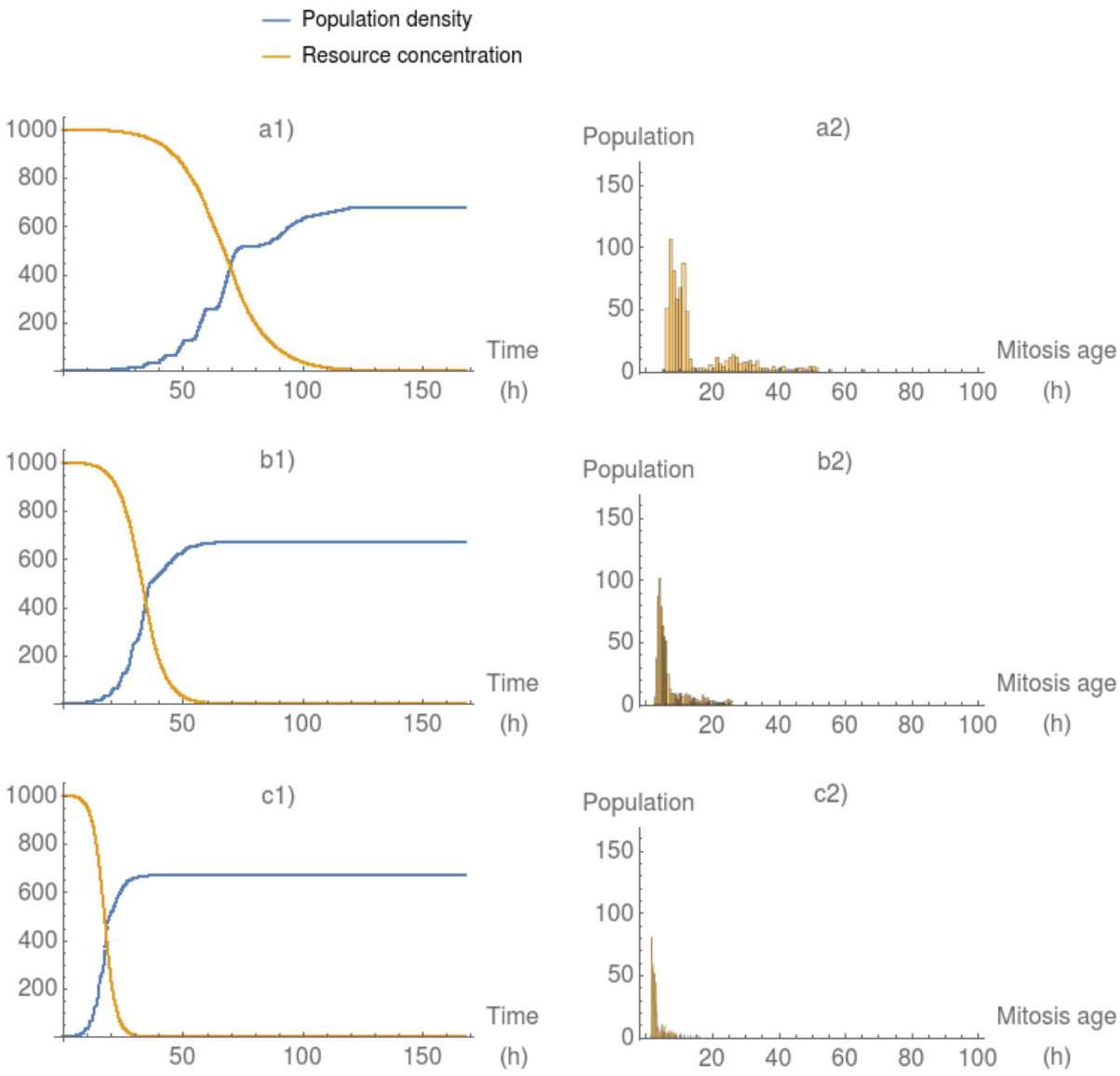

Figure 2.8: Simulations obtained with model equations (2.9) and (2.12) for the evolution of a population of cells feeding off 1 nutrient during 168 hours (in blue) and for the nutrient (in orange). The parameter λ varied according to the normal distribution $\mathcal{N}(\mu, 2 \times 10^{-4})$; Top: $\mu = 1.5 \times 10^{-4}$; Center: $\mu = 3 \times 10^{-4}$; Bottom: $\mu = 6 \times 10^{-4}$.

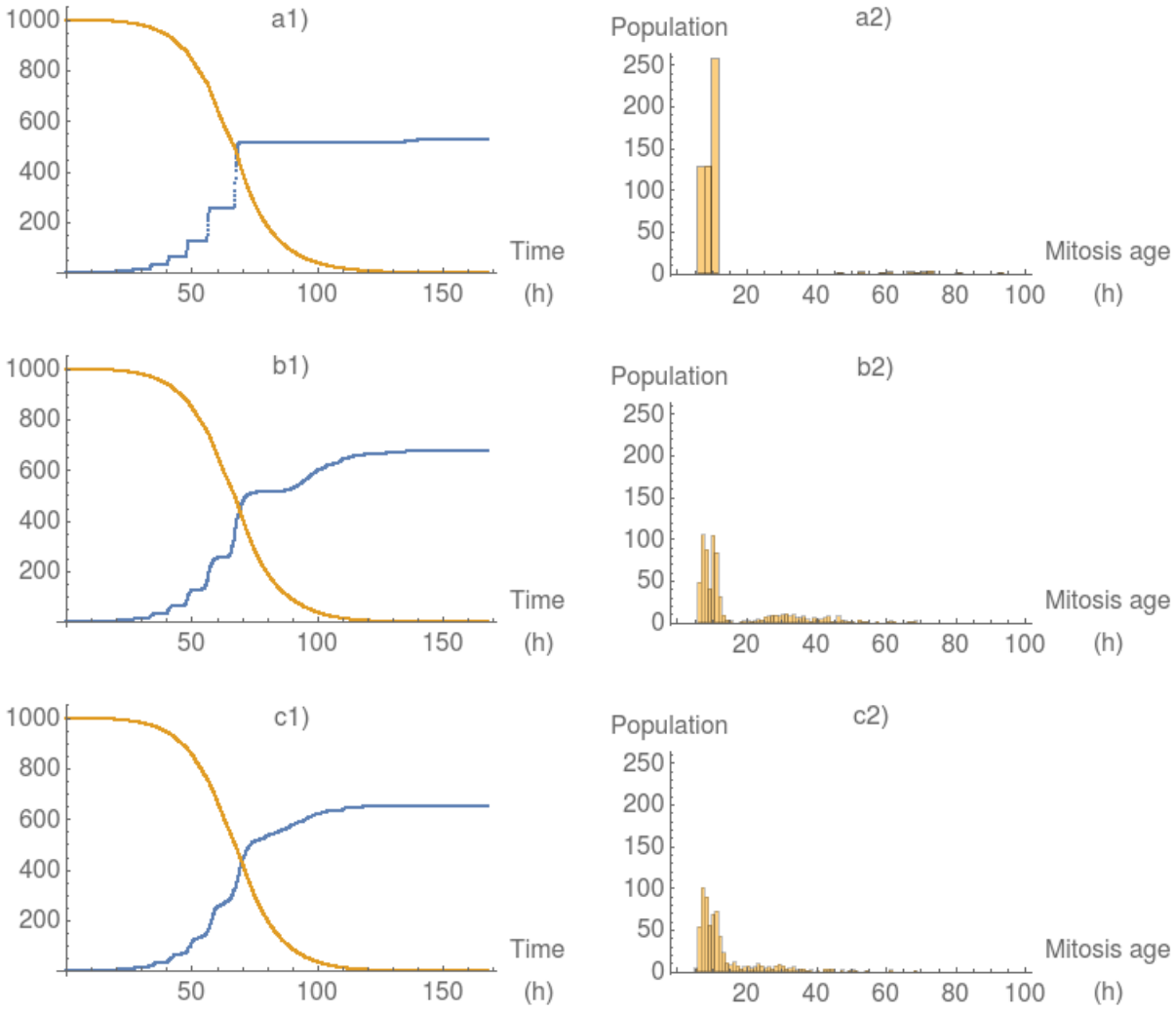

Figure 2.9: Simulations with model equations (2.9) and (2.12) for the evolution of a population of cells feeding off 1 nutrient during 168 hours (in blue) and for the nutrient (in orange). The parameter λ varied according to the normal distribution $\mathcal{N}(1.5\times10^{-4},\sigma)$; Top: $\sigma = 10^{-5}$; Center: $\sigma = 10^{-4}$; Bottom: $\sigma = 10^{-3}$.

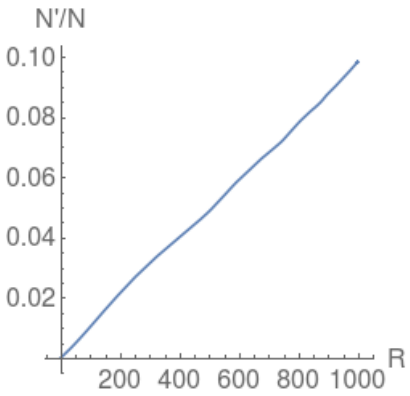

Figure 2.10: $\frac{1}{N}\frac{dN}{dt}$ vs $R(t)$ from the simulated data for the evolution of a nutrient concentration and the population of cells starting with 1 cell feeding off that nutrient, during 168 hours; The parameter λ varied according to the normal distribution with parameters $\mu = 1.5 \times 10^{-4}$ and $\sigma = 2 \times 10^{-4}$. The fit of the curve gives a linear relation $y = 10^{-4}x$ with $\chi^2 = 0.0004$.

In the case of synchronized cultures it is still possible to identify a linear relation between the population growth and the amount of resource (see figure 2.11).

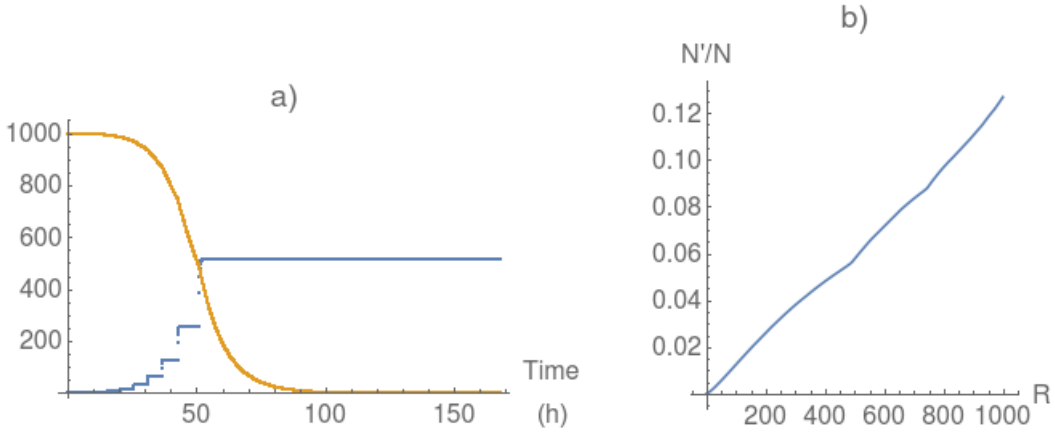

Figure 2.11: a) Evolution of a nutrient concentration and the population of cells feeding off that nutrient, during 168 hours and $\lambda = 2 \times 10^{-4}$; b) The curve shows the relation between the population growth $\frac{1}{N}\frac{dN}{dt}$ and the resource $R(t)$ from the simulated data; The fit of the curve gives a linear relation $y = 6 \times 10^{-5}x$ with $\chi^2 = 0.08$.

From the previous analysis of the logistic and the Monod models we arrive to different relations between the normalized population growth and the amount of resource, equations (1.9) and (1.11). Figure 2.12 demonstrates that the relation between the normalized population growth and the resource concentration is linear when using the Mass action law approach, and non-linear with the Monod function. Thus, under our assumptions, we obtain linear relation 2.11 and the correct model is the logistic.

However, to test our hypothesis, and understand the relation between the Mass Action Law and the Monod model, it is necessary to perform empirical measurements and see how they relate to the corresponding growth curves obtained from these models.

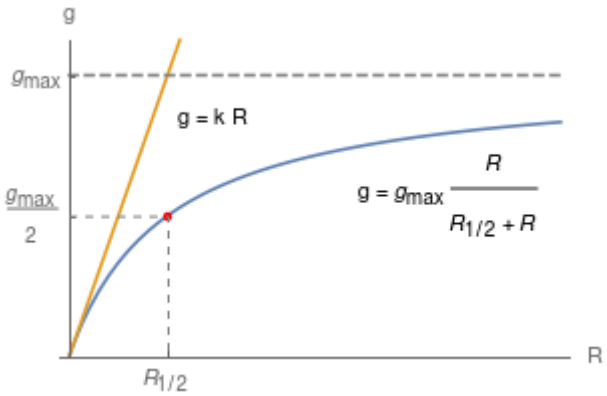

Figure 2.12: Comparison of the relation between the normalized growth rate of a population and the amount of resource still available, in the case of a logistic function (in orange) and of the Monod function (in blue).

2.4 First Experiment and calibration

In this experiment, we grow a culture of *E. coli* in a liquid medium containing glucose ($C_6H_{12}O_6$) and measure the density over time using a spectrometer. As the bacteria multiply, there will be an increase in the density of the solution that contains them. Using this technique, the light that travels through the solution will be partially absorbed by it, and the emitted and transmitted intensities are measured at the wavelength of 600nm to compute a transmittance ratio.

We gather all the data of the time and correspondent optical densities taken during the growth, and then try to test how the empirical Monod model (1.11) and the logistic model obtained from first principles using mass action law approach (1.8) compare with the real growth curves constructed from the data.

Materials:

- Incubator
- Temperature controlled shaker
- Multiskan spectrophotometer
- Bioscreen spectrophotometer
- Scale
- Bunsen burner
- Petri-dishes (approximate dimensions: diameter 8.8 cm, height 1.5 cm)
- 200 µL pipette and pipette tips
- 96-well plates
- Eppendorf tubes
- *E. coli* M61655
- Agar
- Minimal media
- Pure glycerol
- Pure glucose

Procedure:

For the calibration of the model in 2.3, mitosis controlled by consumption of a nutrient and enzymes, we grew a culture of the bacteria *E. coli* MG1655[1].

The *E. coli* were previously storaged in a freezer at -80°C. We transferred a sample of *E. coli* to a previously prepared petri-dish containing approximately 20 ml of solid minimal media[2] with 0.4% glycerol and took them to an incubator at 37°C to stay over night ($\sim$12 h).

On the second day we prepared a 96-well plate with 200 µL of minimal media with 0.20% glycerol in 9 wells. We chose 3 colonies of the *E. coli* petri dish and placed

[1] MG1655 is a strain of *E. coli* that carries few mutations comparatively to the others and thus guarantees a certain consistency in the population behavior.

[2] Minimal media is a solution containing 11.28g of M9 salts, 2mL of $MgSO_4$ 1M, 100µL of $CaCl_2$ 1M and 20mL of a 20% carbon source (0.4% final) per liter of Mili-Q (ultra pure) water; M9 is a mix of 33.9g/L Na_2HPO_4, 15g/L KH_2PO_4, 5g/L NH_4Cl and 2.5g/L NaCl.

3 samples of each culture into the previous wells. The 96-well plate was put in a temperature controlled shaker at low speed ($\sim 10^2$ rpm) and 37°C for the cultures to grow over night ($\sim$12h).

On the third day, the 96-well plate was taken out of the shaker and placed in a multiskan to read the optical densities. This was done to guarantee that the optical densities of the biological (from the different cultures) and technical (from the same culture) copies were all similar and in the appropriate range to start the main growth. All measurements can be consulted in appendix A3.

After the reading, we transferred the cultures to separate eppendorf tubes and prepared a glucose medium of minima media with glucose with concentrations 0.400%, 0.200%, 0.100%, 0.050%, 0.025% and 0.001% for the actual growth in study. We distributed the solutions and cultures according to the configuration in figure 2.13.

We inserted the 96-well plate in a bioscreen for the population to grow for 36 hours while monitoring the Optical Densities every 20 minutes and collected all the data.

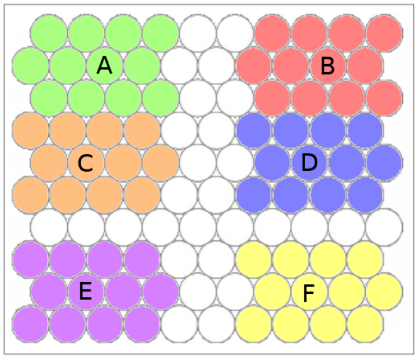

Figure 2.13: Configuration of the bioscreen plate; Each colored set has 20.0 µL of culture 1 in the 1st row, of culture 2 in the 2nd and of the culture 3 in the 3rd mixed with 180.0 µL of minimal media and glucose in concentrations A: 0.400%, B: 0.200%, C: 0.100%, D: 0.050%, E: 0.025% and F: 0.010%.

Results and analysis:

Figure 2.14 shows the Optical Densities obtained during the growth of culture 2 in 0.400% glucose (all the other growth curves, using different cultures and glucose concentrations are present in the Appendix A3). To compare the compatibility of the logistic and Monod models with the data, we took the Optical Densities of the first 750 minutes of the growth, and tested the goodness of fit of equations (1.8) and (1.11) using the Pearson's χ^2 and the Spearman's rank correlation tests. An example of the methods used can be found in the Appendices A4 and A5.

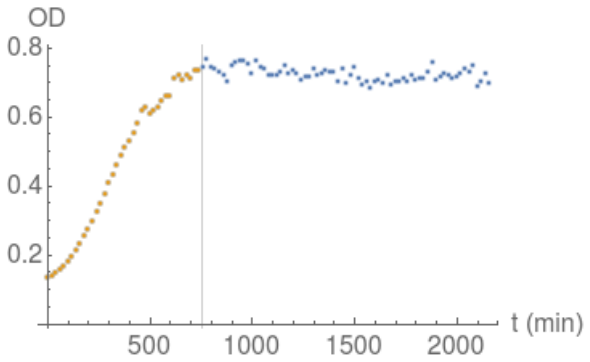

Figure 2.14: Growth curve of *E. coli* population from culture 2 in the presence of minimal media with 0.400% glucose. The initial region in orange will be used for fitting.

However, since we only have data from the Optical Densities, proportional to $N(t)$, and have no information of $R(t)$, we need to write equation (1.11) explicitly.

By Monod's idea of conversion of nutrient into biomass, [3], we have

$$\frac{dN}{dt} = -k\frac{dR}{dt}, \tag{2.15}$$

from which

$$N(t) - N(0) = -k[R(t) - R(0)]. \tag{2.16}$$

Rearranging equation (2.16) we get that

$$R(t) = R(0) - \frac{N(t) - N(0)}{k}. \tag{2.17}$$

Combining equation (1.11) with (2.17) we obtain

$$\frac{1}{N}\frac{dN}{dt} = g_{max}\frac{R(0) - [N(t) - N(0)]/k}{R_{1/2} + R(0) - [N(t) - N(0)]/k}. \tag{2.18}$$

We can write the proportionality between the optical density and the number of bacteria as

$$OD(t) = qN(t) \tag{2.19}$$

in which q is a positive real constant.

Substituting this relation in the model equation of (2.18), we obtain

$$\frac{q}{OD}\frac{d(OD/q)}{dt} = g_{max}\frac{R(0) - [OD(t)/q - OD(0)/q]/k}{R_{1/2} + R(0) - [OD(t)/q - OD(0)/q]/k}. \tag{2.20}$$

$$\iff \frac{1}{OD}\frac{d(OD)}{dt} = g_{max}\frac{R(0) - \tilde{k}[OD(t) - OD(0)]}{R_{1/2} + R(0) - \tilde{k}[OD(t) - OD(0)]}$$

where $\tilde{k} = 1/(kq)$.

The same can be done with the first model equation of (1.8),

$$N(t) = \frac{C\ e^{kCt}}{\frac{C}{N(0)} - 1 + e^{kCt}} \iff \frac{OD(t)}{q} = \frac{C\ e^{kCt}}{\frac{C}{OD(0)/q} - 1 + e^{kCt}}$$

$$\iff OD(t) = \frac{qC\ e^{kCt}}{\frac{qC}{OD(0)} - 1 + e^{kCt}} = \frac{(qC)\ e^{\frac{k}{q}(qC)t}}{\frac{(qC)}{OD(0)} - 1 + e^{\frac{k}{q}(qC)t}} \tag{2.21}$$

$$\iff OD(t) = \frac{m\ e^{b\,m\,t}}{\frac{m}{OD(0)} - 1 + e^{b\,m\,t}}$$

in which $b = qC$ and $m = k/C$.

In both cases we see that $OD(t)$ and $N(t)$ take the same form.

Figure 2.15 shows the comparison between the fitting of the model equations (2.21) and (2.20).

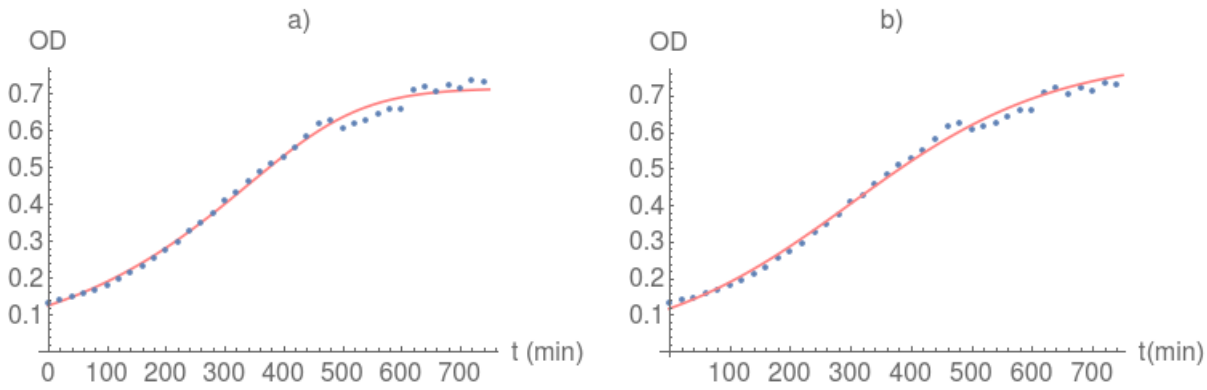

Figure 2.15: a) Initial data from figure 2.14 and respective fit using the Monod function. The fitted parameters for the equation (2.20) have results $R(0) = 0.210$, $R_{1/2} = 0.126$, $g_{max} = 0.007\,\text{min}^{-1}$, $\tilde{k} = 0.357$ and $OD(0) = 0.124$ with a $\chi^2 = 0.016$ and $\rho_r = 0.996$; b) Initial data from figure 2.14 and respective fit using the Mass action law approach. The fitted parameters for the equation (2.21) have results $b = 0.007$, $m = 0.808$, $OD(0) = 0.116$, with a $\chi^2 = 0.279$ and $\rho_r = 0.996$.

The fits were done by first establishing the parameters visually and then by setting increasingly closer randomly generated values in order to lower the χ^2 parameter for 10^4 iterations (see appendices A4 and A5).

Although both models provide very good approximations to the data ($\chi^2 \ll 1$ and $\rho_r \approx 1$), as expected, the model with the most parameters will be easier to fit and have the smaller χ^2. Therefore, it is impossible to distinguish between the two outcomes

and say which model is the valid one by this analysis. The only way to present a solid justification for either of the models is to make independent measurements of the Optical Densities of the bacteria and the nutrient concentrations and do the test presented in figure 2.12.

2.5 Analysis of existing data

In 2011 [10], Mostovenko and his colleagues designed an experiment consisting in a culture of *E. coli* supplied by a medium containing both glucose and lactose to study the production of proteins involved in the adaptation of bacteria when consuming a different nutrient than before, during a diauxic growth.

In figure 2.16 we have the graph from [10] containing the *E. coli* growth rate, showing diauxic shift, against the glucose consumption curve.

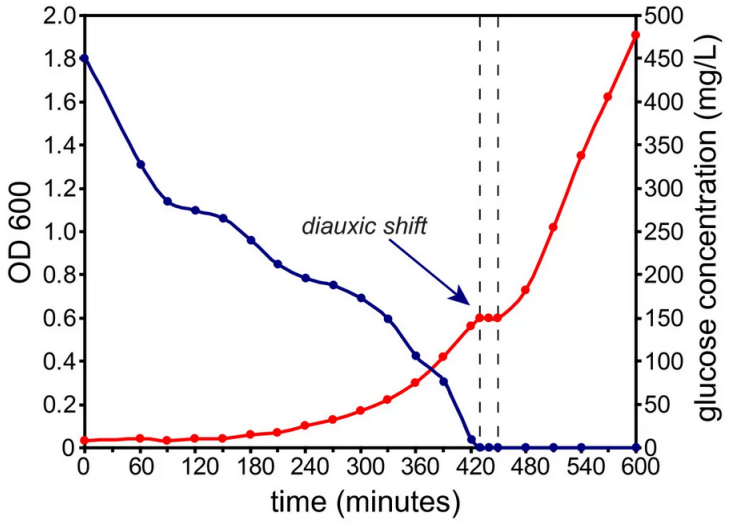

Figure 2.16: Measured optical densities in red and glucose concentrations decreasing in blue. The optical density is proportional to the number of bacteria present in the media.

We collected the data from his work and used it to make a primary analysis of the relation between the population growth and the nutrient evolution curves. We obtained the data of the Optical Densities and glucose concentrations up until the 420 minutes, where the diauxie transition begins.

It is possible to identify a quasi-linear region in the initial growth of figure 2.17, until 100 mg/mL, that contrasts with the Monod model. In fact, the curve has the opposite concavity. Still, the precision of the measured optical densities and sugar concentrations does not seem sufficient to make this analysis conclusive. Therefore, it would be necessary to elaborate an experiment where the *E. coli* grow in a single

sugar medium and take measurements of the population and sugar Optical Densities with a great level of precision and then repeat this same study.

The first region in figure 2.17 precedes another quasi-linear section with negative normalized growth, which is an indication that bacteria suffer a toxicity effect in the presence of high concentrations of nutrient. In fact, this effect has been used to explain the lag phases in diauxic shifts, [23].

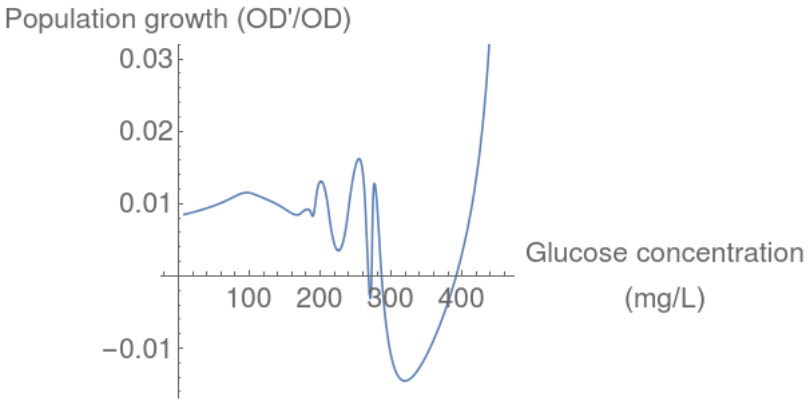

Figure 2.17: Curve of the OD'/OD vs glucose concentration calculated from the first 420 minutes of data in figure 2.16 from the Mostovenko work [10].

2.6 Third model: Mitosis controlled by the consumption of one nutrient and including toxicity

In this next model, we consider that a carbon source (glucose) G is transformed by an enzyme, E, at a constant rate k_1, creating an enzyme-carbon complex, X, (the inverse reaction also occurs, at a rate k_{-1}), that is then transformed into an absorbable energy resource R at rate k_2, and the enzyme is released — this enzymatic mechanism is represented by the Michaelis-Menten kinetic diagram (2.22). The resource R will then be absorbed by N bacteria at a constant rate k_3, and the bacteria will reproduce (2.23). When there is too much glucose in the medium it becomes toxic to the *E. coli*, [22], repressing their growth (represented by $\emptyset$) in (2.24).

$$\begin{cases} G + E \underset{k_{-1}}{\overset{k_1}{\leftrightarrows}} X \xrightarrow{k_2} E + R, & (2.22) \\ R + N \xrightarrow{k_3} 2N, & (2.23) \\ G + N \xrightarrow{k_4} \emptyset. & (2.24) \end{cases}$$

According to the mass action law, the time evolution equations become

$$\begin{cases} G' = k_{-1}X - k_1GE - k_4GN, \\ E' = k_{-1}X - k_1GE + k_2X, \\ X' = -k_{-1}X + k_1GE - k_2X, \\ R' = k_2X - k_3RN, \\ N' = k_3RN - k_4GN, \end{cases} \tag{2.25}$$

from which we can obtain the conservation laws

$$\begin{cases} G' - E' + R' + N' = 0 \\ E' + X' = 0 \end{cases} \tag{2.26}$$

$$\implies \begin{cases} G - E + R + N = c_1 \\ E + X = c_2 \end{cases}.$$

where c_1 and c_2 are positive constants.

As initially there are no enzyme-nutrient complexes yet formed, $X(0) = 0$. Moreover, there is no transformed nutrient in the beginning, $R(0) = 0$. Thus,

$$c_1 = G(0) - E(0) + N(0) \tag{2.27}$$

and the previous equations can be written as

$$\begin{cases} G - E + R + N = G(0) - E(0) + N(0) \\ E + X = E(0) \end{cases}$$

$$\implies \begin{cases} E = G + R + N - [G(0) - E(0) + N(0)] \\ X = E(0) - E \end{cases}$$

$$\implies \begin{cases} E = [G - G(0)] + R + [N - N(0)] + E(0) \\ X = [G(0) - G] - R + [N(0) - N] \end{cases}. \tag{2.28}$$

Substituting the above equations (2.28) in (2.25), we obtain the system of equations

$$\begin{cases} G' &= k_{-1}\Big\{ [G(0)-G] - R + [N(0)-N] \Big\} \\ &\quad +k_1 G\Big\{ [G(0)-G] - R + [N(0)-N] - E(0) \Big\} - k_4 GN, \\ R' &= k_2 \Big\{ [G(0)-G] - R + [N(0)-N] \Big\} - k_3 RN, \\ N' &= k_3 RN - k_4 GN, \end{cases} \tag{2.29}$$

A steady state solution of the system of equations (2.29) can be solved numerically by setting the initial conditions

$$\begin{cases} G(0) = G_0 \\ E(0) = E_0 \\ N(0) = N_0 \end{cases}, \tag{2.30}$$

where G_0, E_0 and N_0 are chosen constants.

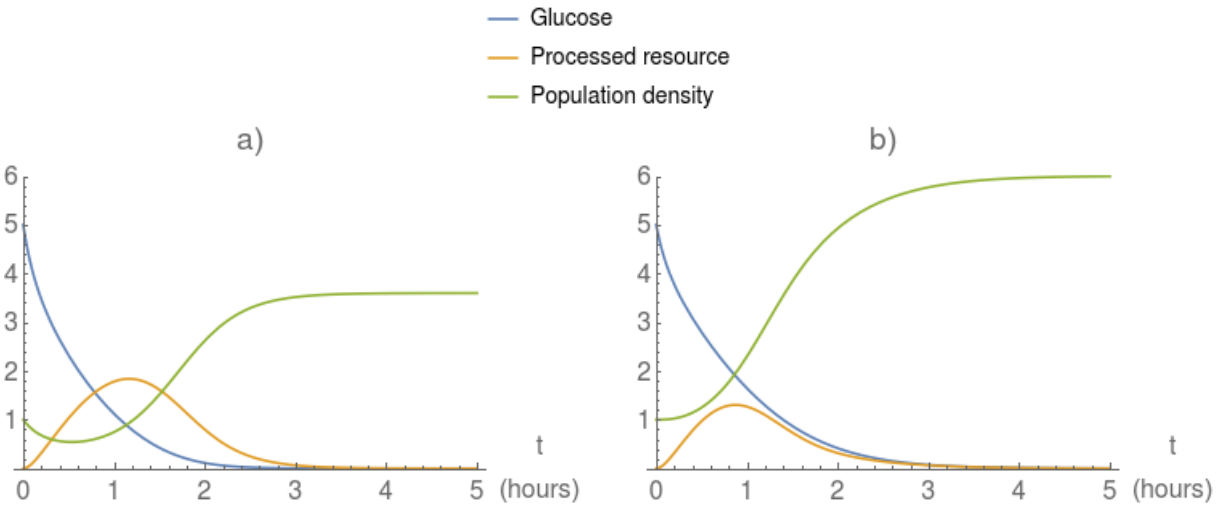

Figure 2.18: Simulations obtained with the steady state model equations (2.29) and (2.30), as a function of t, for $t_{max} = 5h$, $G_0 = 5.0$, $E_0 = 2.0$, $N_0 = 1.0$, $k_{-1} = 0.1$, $k_1 = 1.0$, $k_2 = 3.0$, $k_3 = 1.0$ and a) $k_4 = 0.5$ b) $k_4 = 0.0$.

Figure 2.18 shows a simulation of a population of cells feeding off one type of nutrient (which we called glucose for identification purposes only), and the corresponding nutrient concentration over time, along with the amount of processed resource by the cells. In a) it is possible to identify a region in the beginning of the growth where the population density drops while the nutrient concentration is the highest and the re-

source is being processed very quickly. Based on the studies of G. Lambert and E. Kussell, [22], and B. Cerulus et al., [23], this behavior is expected whenever the nutrient concentration exceeds a certain threshold. As a consequence of this initial toxicity effect, the final population density reached is lower.

2.7 Forth model: Mitosis controlled by the consumption of two nutrients and including toxicity

In this model we include a possible mechanism behind the occurrence of diauxies. This model describes the consumption of two different carbon sources (G and S) by a population of cells (N), with the same enzymatic process as before, the enzymes (E_1 and E_2) help to transform the nutrients into the corresponding complexes (X_1 and X_2) and successively into metabolizable resource R, in addition to the reproduction of individuals in the presence of resource and two different toxicities associated with each carbon source.

$$\begin{cases} G + E_1 \underset{k_{-1}}{\overset{k_1}{\leftrightarrows}} X_1 \overset{k_3}{\to} E_1 + R, \\ S + E_2 \underset{k_{-2}}{\overset{k_2}{\leftrightarrows}} X_2 \overset{k_4}{\to} E_2 + R, \\ R + N \overset{k_5}{\to} 2N, \\ G + N \overset{k_6}{\to} \emptyset, \\ S + N \overset{k_7}{\to} \emptyset \end{cases} \tag{2.31}$$

By the mass action law, the time evolution equations are

$$\begin{cases} G' = k_{-1}X_1 - k_1 G E_1 - k_6 G N \\ S' = k_{-2}X_2 - k_2 S E_2 - k_7 S N \\ E_1' = (k_{-1} + k_3)X_1 - k_1 G E_1 \\ E_2' = (k_{-2} + k_4)X_2 - k_2 S E_2 \\ R' = k_3 X_1 + k_4 X_2 - k_5 R N \\ N' = k_5 R N - k_6 G N - k_7 S N \end{cases}, \tag{2.32}$$

from which we can obtain the conservation laws

$$\begin{cases} G' + S' - E_1' - E_2' + R' + N' = 0 \\ E_1' + X_1' = 0 \\ E_2' + X_2' = 0 \end{cases}$$

$$\implies \begin{cases} G + S - E_1 - E_2 + R + N = c_1 \\ E_1 + X_1 = c_2 \\ E_2 + X_2 = c_3 \end{cases} . \tag{2.33}$$

where c_1, c_2 and c_3 are positive constants.

As initially there are no enzyme-nutrient complexes yet formed, $X_1(0) = X_2(0) = 0$. Moreover, there is no transformed nutrient in the beginning, $R(0) = 0$. Thus,

$$c_1 = G(0) + S(0) - E_1(0) - E_2(0) + N(0) \tag{2.34}$$

and the previous equations can be written as

$$\begin{cases} G + S - E_1 - E_2 + R + N = G(0) + S(0) - E_1(0) - E_2(0) + N(0) \\ E_1 + X_1 = E_1(0) \\ E_2 + X_2 = E_2(0) \end{cases}$$

$$\implies \begin{cases} E_2 = G + S - E_1 + R + N - [G(0) + S(0) - E_1(0) - E_2(0) + N(0)] \\ X_1 = E_1(0) - E_1 \\ X_2 = E_2(0) - E_2 \end{cases}$$

$$\implies \begin{cases} E_2 = [G - G(0)] + [S - S(0)] + R + [N - N(0)] - [E_1 - E_1(0)] + E_2(0) \\ X_1 = E_1(0) - E_1 \\ X_2 = [G(0) - G] + [S(0) - S] - R + [N(0) - N] - [E_1(0) - E_1] \end{cases} \tag{2.35}$$

Substituting the above equations (2.35) in (2.32), we obtain the system of equations

$$\begin{cases} G' &= k_{-1}\left[E_1(0) - E_1\right] - k_1 G E_1 - k_6 G N \\ \\ S' &= k_{-2}\Big\{ \left[G(0) - G\right] + \left[S(0) - S\right] - R + \left[N(0) - N\right] - \left[E_1(0) - E_1\right] \Big\} \\ &\quad + k_2\, S\Big\{ \left[G(0) - G\right] + \left[S(0) - S\right] - R + \left[N(0) - N\right] - \left[E_1(0) - E_1\right] - E_2(0) \Big\} \\ &\quad - k_7\, S N \\ \\ E_1' &= (k_{-1} + k_3)\left[E_1(0) - E_1\right] - k_1 G E_1 \\ \\ R' &= k_3\left[E_1(0) - E_1\right] \\ &\quad + k_4\Big\{ \left[G(0) - G\right] + \left[S(0) - S\right] - R + \left[N(0) - N\right] - \left[E_1(0) - E_1\right] \Big\} - k_5 R N \\ \\ N' &= k_5 R N - k_6 G N - k_7 S N \end{cases}, \tag{2.36}$$

Equations (2.36) can be solved numerically provided initial conditions

$$\begin{cases} G(0) = G_0 \\ S(0) = S_0 \\ E_1(0) = E_{10} \\ E_2(0) = E_{20} \\ N(0) = N_0 \end{cases} \tag{2.37}$$

where G_0, S_0, E_{10}, E_{20} and N_0 are chosen constants.

Figure 2.19 shows two simulations of a population of cells feeding off two different types of nutrient (which we called glucose and Sorbitol for identification purposes only), and the corresponding nutrient concentrations over time. As in figure 2.18a), it is possible to identify a region in the beginning of the growth where the population density drops while the nutrient concentrations are at the highest. After that transition, the population grows and reaches a plateau before continuing to grow.

Note that within this setup, the diauxie appears before the extinction of the first nutrient, the glucose, opposed to what Monod previously believed.

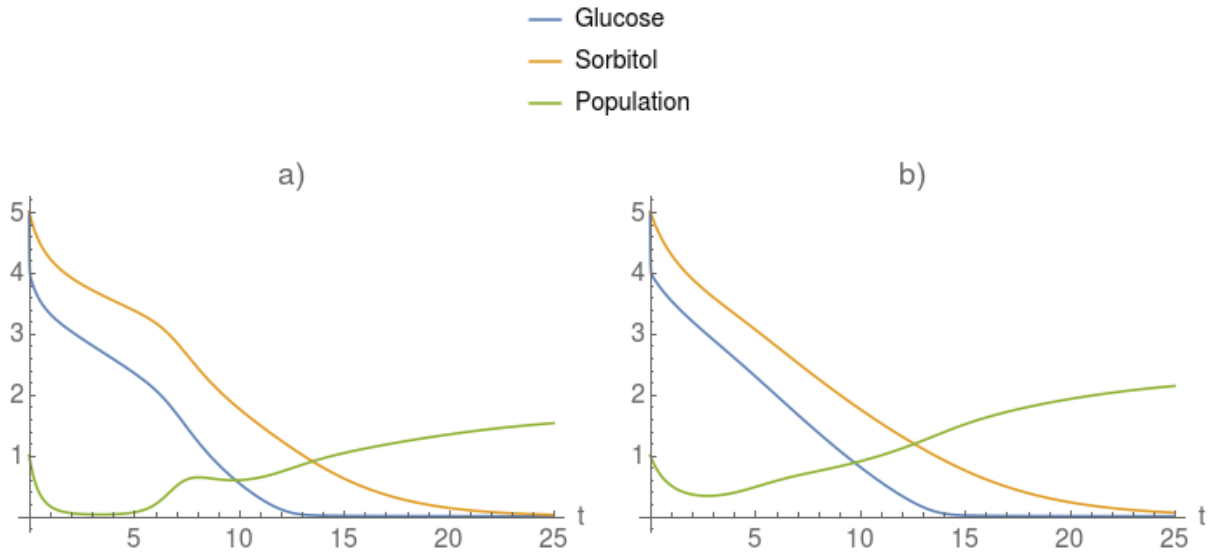

Figure 2.19: Simulations obtained with the steady state model equations (2.36) and (2.37) as a function of t for $t_{max} = 25h$, $G_0 = 5$, $\alpha_0 = 5$ $E_{10} = 1$, $E_{20} = 1$, $N_0 = 1.0$, $k_{-1} = 0.1$, $k_1 = 20$, $k_{-2} = 0.01$, $k_2 = 0.1$, $k_3 = 0.2$, $k_4 = 0.2$, $k_5 = 2$ and a) $k_6 = 0.3$ and $k_7 = 0.2$ b) $k_6 = 0.1$ and $k_7 = 0.1$.

2.8 Second experiment proposal

Bacteria take time to adapt in order to eat a sugar that they have no memory of. When bacteria eat a sugar that they already know, their starting growth happens sooner and faster. However, to process some nutrients bacteria can transform the carbon source into another though enzymatic processes. Since we want to search for glucose-sorbitol diauxies, we should use a different sugar for the pre-culture, that is not connected through natural enzymatic processes, for example mannose, in order to avoid favoring one of the growths.

It is important to first obtain the growth curves of the bacteria consuming the sugars separately, in the same setup as the experiment that will be done with both sugars, to know the duration of the initial lag phases, the population maximum and the time necessary to reach it.

Materials:

- Multiskan spectrophotometer
- Incubator
- Centrifuge
- Scale
- Timer or clock
- Flasks
- 5mL and 10mL pipettes and pump
- 20µL, 200µL and 1000µL pipettes and pipette tips
- Normal and deep 96-well plates

- Glass beads
- *E. coli* M61655
- Lysogeny broth[3] agar plates
- Minimal media
- PBS buffer[4]
- Pure mannose
- Pure glucose
- Pure sorbitol
- Glucose and sorbitol Sigma-Aldrich assay kits (MAK263 and MAK010)

Part 1 procedure:

Grow an *E. coli* sample from the freezer in an Lysogeny broth agar plate for 24 hours in an incubator. Prepare flasks with a 50mL solution of minimal media with 0.2% mannose and 100mL solutions of minimal media with 0.1% glucose and of minimal media with 0.1% sorbitol.

The next day, put 15ml of a 0.2% mannose solution in three 25 mL tubes using the 10mL and 5mL pipettes. Select two *E. coli* cultures from the Lysogeny broth agar plate and transfer them separately (with a small pipette) into two of the tubes containing the mannose solution using a small pipette. The third tube is a negative control, used to make sure that the system is not contaminated with any other organisms. Label the tubes with the respective contents and place them in the shaker at 37°C for 24 hours.

On the following day, take the tubes out from the shaker and use them to prepare 10-fold dilutions to determine the Optical Densities and number of cells.

To know the starting number of cells after the pre-culture growth we need to relate the Optical Densities of some samples with the number of cultures in the same amount. By platting a small quantity of cells in an agar plate and letting them multiply in the incubator, it is possible to see scattered cultures, each originated from a single cell.

Start by distributing 200µL of each solution in the first row (or column) of a 96-well plate and 180µL of minimal media to the next 7. Create the dilutions by successively adding and mixing 20µL of the previous well to the next using a pipette, leaving the last well with only minimal media for the blank. Read the 96-well plate in the multiskan and follow the optical density over time.

Similarly, prepare six 10-fold dilutions in a deep 96-well plate using 50µL of the solution to 450µL of PBS. Plate 100µL of each 10^{-4}, 10^{-5} and 10^{-6} solutions spreading the liquid with the glass beads. Put the agar plates in the incubator for the cultures to grow until they are sizable enough to be seen. When possible, count the number of cultures in each plate and plot them against the corresponding Optical Densities with the blank subtracted; the graph should be a linear tendency.

To start the culture on the single sugars, wash the cells by centrifuging, removing the supernatant and re-suspending them in minimal media. Then transfer 15mL of the 0.1% glucose solution into four 25mL tubes and add 150µL of the washed cells to three

[3] Solution containing 10 g/L peptone, 5 g/L yeast extract, 10 g/L NaCl (and 15 g/L agar for solid medium).
[4] PBS is a Phosphate-buffered saline solution used to stabilize the reactions by maintaining a constant pH.

of them, leaving the last as a control; do the same with the sorbitol solution. Repeat dilutions, Optical density readings and plating to double check the starting number of cells. Finally, label all the tubes and start the timer for 1 hours before taking them to the shaker at 37°C.

Prepare the Sigma-Aldrich assay kits solutions to measure the sugar concentrations, following the manual instructions. Every next hour remove the tubes from the shaker, take 100µL samples of all the tubes to a 96-well plate and read the Optical Densities with the multiskan. Then, following the assay kits instructions, centrifuge another sample to take a portion of the supernatant and mix the assay kits prepared solutions. Finally, read the sugar concentrations in the multiskan. Plot the Optical Densities vs time as the experiment goes to see the growth curve and detect its ending.

Part 2 procedure:

For the second part of this experiment we propose to repeat the experiment above but using both sugars at the same time instead of just one and take measurements of the culture and sugars Optical Densities to obtain the diauxic curve and the nutrient consumption curves.

Chapter 3

Conclusions

The Monod function is an empirical model describing the relation between the growth of a population of cells and the expense of nutrient it is feeding of. Many modern models are based on the Monod's function. However none has depicted the most essential phenomena — the diauxic growth and toxicity effects — completely or accurately enough.

We presented alternative models starting with a simple construction, in section 2.2, where the only dependency is on time. There, we simulate the reproduction of cells, in which the mitosis duration is regulated by a stochastic parameter accounting for the memory dependent behavior observed in the experiments of Lambert and Cerelus, [22] [23], yielding a Malthusian curve.

In section 2.3 we consider a real setup, where bacteria have access to a limited amount of nutrient. In this case, the mitosis is triggered by a threshold amount of protein, obtained from the metabolized nutrient, a phenomenon documented by Prescott in 1959, [30]. The construction introduced reproduces sigmoidal curves for the normalized population growth and nutrient concentration. The relation between the two is shown to be linear, in contradiction to the Monod's function. Moreover, it agrees with Verhulst's equation, derived from the Mass action law. The experiment developed at the Instituto Gulbenkian de Ciência, detailed in section 2.4, leaves the possibility open for the fact that a Logistic can be the correct model in this setting. In addition, the normalized growth rate and nutrient concentration from Mostovenko's data, [10], exhibit a similar quasi-linear relation in the section where bacteria are feeding only of glucose, the first nutrient, before the diauxic shift occurs.

To take into account the toxicity phenomenon observed by Lambert, [22], and Cerelus, [23], we created a simple model describing a population feeding off a nutrient, in three parts: nutrient metabolization, cells reproduction and growth inhibition through direct or indirect nutrient interaction. We used the same Mass Action Law method as before to transform the kinetic equations into time dependent differential equations, and solved for the chosen initial conditions. The results indicate that the initial cur-

vature in the evolution of population growth observed and identified as a lag-phase, which can become negative is some circumstances, can be explained by this known toxicity effect and modeled using the law of mass action and only the basic interactions of consumption reproduction and death.

The diauxic shifts, observed when bacteria are presented to two nutrients with different metabolization costs, and consequently rates, translate into a decrease of the population growth regulated by the nutrients expense. Because of this, it is expected that the phenomenon is related to the same toxicity effect. The model of section 2.7 was obtained by a generalization of the previous one, where this time we introduced the enzymatic process of metabolization, reproduction and death for both nutrients. The implementation of the equations achieved with the mass action law method suggest that the diauxic growth arises naturally without the need for an added interaction.

Bibliography

[1] G. Miller; Scott Spoolman, 2012. Environmental Science 13th edition p. 60. (2009).

Insight on what is biodiversity and why it is important, identified species and estimates on the real number.

[2] C. Darwin, The Voyage of the Beagle, 1839.

Journal of observation of species evolution.

[3] Monod J. (1942) Recherches sur la croissance des cultures bactriennes, Hermann, Paris.

First major important mathematical study on the relation between growth rate of bacterial cultures and concentration of nutrient in the medium. Empirical discovery of the diauxic growth.

[4] Anna Posfai, Thibaud Taillefumier, and Ned S. Wingreen, Metabolic Trade-Offs Promote Diversity in a Model Ecosystem , PRL 118, 028103 (2017).

Inclusion of trade-offs and stochastic fluctuations into a resource-competition model in order to explain coexistence of species as we observe in many ecosystems.

[5] Leonardo Pacciani-Mori, Samir Suweis and Amos Maritan, Adaptive consumer-resource models can explain diauxic shifts and the violation of the Competitive Exclusion Principle, Aug. 6, 2018; doi: http://dx.doi.org/10.1101/385724.

Inclusion of adaptative metabolic strategies in a resource-competition model and analysis of their importance in maintaining population equilibrium depending on their time-scales.

[6] T. Escherich, Die Darmbakterien des Suglings und ihre Beziehungen zur Physiologie der Verdauung, 1886.

Discovery of the bacteria *E. coli* by Theodor Escherich.

[7] Escherichia coli Strains and NIH Guidelines, https://blink.ucsd.edu/safety/research-lab/biosafety/nih/e-coli.html, (2017).

Commonly used strains of *E. coli* in biology experiments.

[8] Dick Neal, Introduction to Population Biology, Cambridge Uni. Press., 2004.
Introduction to concepts of biological dynamics: Theories of evolution and natural selection, population growth models, importance of genetics and mutations, demography and interaction between species.

[9] Rui Dilão, Mathematical Models in Population Dynamics and Ecology, 2006
Age dependent population models following the Leslie system of fertility and death probability. Comparison of the Tessier-Monod growth model with the mass action alternative.

[10] Ekaterina Mostovenko, André M Deelder and Magnus Palmblad, Protein expression dynamics during Escherichia Coli glucose-lactose diauxie, BMC Microbiology, 2011.
Study on the production of proteins involved in the adaptation of bacteria to consume a different nutrient than before.

[11] T. R. Malthus, An Essay on the Principle of Population, 1798.
Book on populational dynamics; Formulation of the exponential growth model.

[12] P. Waage, P and C. M. Guldberg (1864), ”Studier over Affiniteten”, Transactions of the Scientific Society in Christiania.
Invention of the Law of mass action

[13] P. F. Verhulst, Recherches Mathematiques sur la Loi D’Accroissement de La Population, 1845
Mathematical models based on population data; Derivation of the logistic growth model.

[14] R. MacArthur, Theoretical Population Biology 1, 1 (1970).
First mathematical model of major importance describing a set of individuals competing for the same set of resources.

[15] Gause, Georgii Frantsevich (1934). The Struggle For Existence (1st ed.). Baltimore: Williams & Wilkins.
Formulation of the Gause’s Law.

[16] G. Hardin et al., Science 131, 1292 (1960).
Formulation of the Competitive Exclusion Principle.

[17] Hutchinson, G. E. (1961) The paradox of the plankton. American Naturalist 95, 137-145.
Plankton can grow in situations of limited resources, contrary of what is expected.

[18] Robert MacArthur and Edward Wilson (1963) An Equilibrium Theory of Insular Zoogeography.

Model that shows the possibility of an equilibrium between immigration of new species and extinction of the present ones.

[19] Robert MacArthur and Edward Wilson, The Theory of Island Biogeography (Princeton University Press, 1967)

Studies on the diversity of species considering the geographic area, competition and colonization.

[20] S. P. Hubbell, The Unified Neutral Theory of Biodiversity and Biogeography (Princeton University Press, Princeton, 2001).

Attempt to explain biodiversity in ecological communities by considering stochastic effects on populations.

[21] Erickson, D., Schink, S., Patsalo, V. et al. A global resource allocation strategy governs growth transition kinetics of Escherichia coli. Nature 551, 119123 (2017). https://doi.org/10.1038/nature24299

Relation between the growth rate of E. coli and its RNA and protein.

[22] G. Lambert and E. Kussell, Memory and Fitness Optimization of Bacteria under Fluctuating Environments, 2014, PLOS Genetics.

Existence of a non-genetic memory in the process of mitosis when adapting to the consumption of different nutrients.

[23] B. Cerulus et al., Transition between fermentation and respiration determines history-dependent behavior in fluctuating carbon sources, 2018, eLife.

Molecular mechanisms related to bacterial adaptation between alternating nutrients; Correlation of the duration of lag phases and duration of permanence in nutrients.

[24] Rubinow, Mathematical Problems in the Biological Sciences, 1973.

Population growth models with applications on the eukaryote Tetrahymena.

[25] Patrick H. Leslie (1942) On the use of matrices in certain population mathematics

Human population growth models formulated from phenomenological observations.

[26] Analyse Mathematique. Sur les probabilits des erreurs de situation d'un point, 1844, Mem. Acad. Roy. Sci. Inst. France, Sci. Math, et Phys., p. 255-332.

Derivation of the Pearson correlation coefficient.

[27] Karl Pearson, 1900, ”On the criterion that a given system of deviations from the probable in the case of a correlated system of variables is such that it can be reasonably supposed to have arisen from random sampling”, Philosophical Magazine, Series 5.

Formulation of the statistic χ^2 test.

[28] C. Spearman (1904), The Proof and Measurement of Association between Two Things, The American Journal of Psychology.

Formulation of the Spearman ranking correlation coefficient.

[29] Matthew Scott and Terence Hwa, Bacterial growth laws and their applications, Curr Opin Biotechnol. 2011 August ; 22(4): 559565. doi:10.1016/j.copbio.2011.04.014.

Chronological description of discoveries, creation of models and their limitations; open problems.

[30] Prescott, Relation Between Cell Growth and Cell Division, 1959.

Loss of asynchrony in cell cultures; Discovery of a threshold of metabolized protein necessary for cell division.

Appendices

A1 Mitosis controlled by age memory

Simulation of a growth curve and distribution of the mitosis ages of cells feeding off unlimited resource, using the model equation 2.8.

```
σ = 0.1;(* standard deviation of the normal distribution *)
tMax = 40; (* duration of the experiment *)
n0 = 1; (* number of initial cells *)

δ[n_, σ_, dt_] := Round[RandomVariate[
    TruncatedDistribution[{-2 σ, 2 σ}, NormalDistribution[0, σ]], n], dt] ;
 (* variation of the times until for n cells,
chosen with gaussian probabilities of standard
 deviation σ and rounded to the smallest time step dt*)

dt = 0.01; (* time steps *)
T = 3; (* time of reference until mitosis *)

t = 0;
data = {{0, n0}}; (* the simulation starts at t=0, when there are n0 cells *)
a = ConstantArray[0, n0] ; (* age of the first cells *)
A = {}; (* mitosis age *)
Δt = T + δ[n0, σ, dt]; (* first time until mitosis *)

While[t < tMax,
 {Do[
   If[a[[k]] == Δt[[k]], (* if the cell's age reaches the mitosis time *)
    {A = Append[A, a[[k]]];
     (* 'A' saves the time at which mitosis happened *)
     a = Flatten[ReplacePart[a, k → {0, 0}]];
     (* two new ages substitute the age before *)
     Δt = Flatten[ReplacePart[Δt, k → Δt[[k]] + δ[2, σ, dt]]];}
   ],
   {k, Length[a]}]; (* do it for all the cells *)
  data = Append[data, {t, Length[a]}];
  (* 'data' saves the number of cells in that moment *)
  a = a + dt;}; (* age increases *)
 t = t + dt]; (* next time step *)
```

In[95]:=
```
evl1 = ListPlot[Take[data, 2002],
  AxesLabel → {"Time\n(h)", "Population density"}, LabelStyle → Directive[15]]
```

Out[95]=

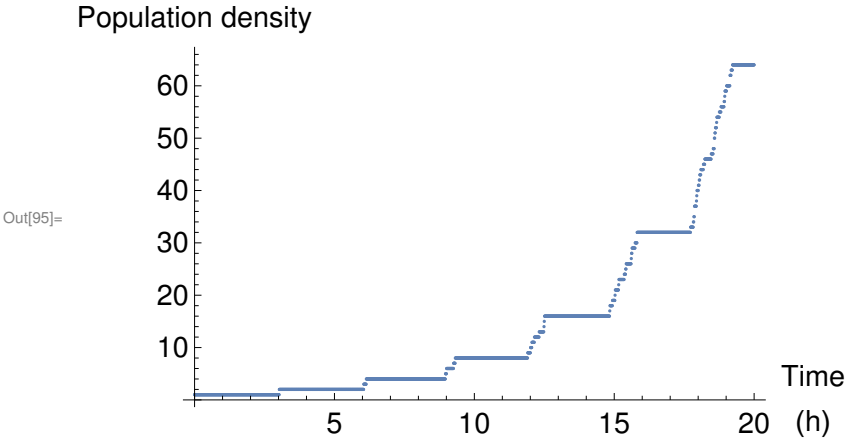

In[94]:=
```
evl2 = ListPlot[data,
  AxesLabel → {"Time\n(h)", "Population density"}, LabelStyle → Directive[15]]
```

Out[94]=

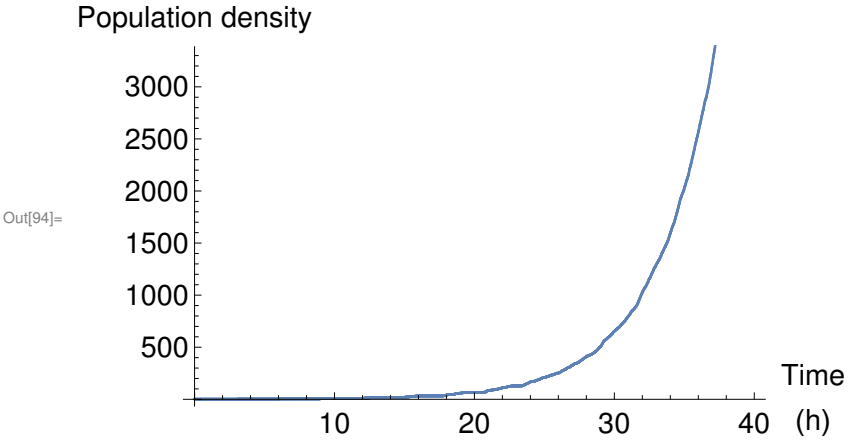

In[93]:=
```
hst = Histogram[A, 100, AxesLabel → {"Mitosis age\n(h)", "Population density"},
  LabelStyle → Directive[15]]
```

Out[93]=

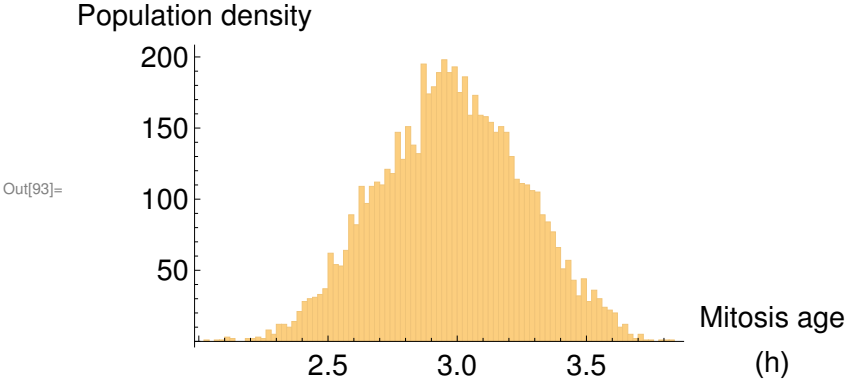

Fitting of the simulation of a growth curve of cells feeding off unlimited resource, using the model equation 2.8, to a power function.

Data simulation

In[21]:=
```
Clear[t, k, c, f]

T = 3.51; (* time until mitosis *)
tMax = 78; (* duration of the experiment *)
n0 = 1; (* initial number of bacteria *)
dt = 0.01; (* time steps *)
t = 0; (* begining of the experiment *)
data = {};
kMax = Floor[tMax / T]; (* number of generated data points *)
n = n0; (* initial number of bacteria *)
k = 0; (* for counting the number of data points *)

While[t < tMax,
  If[k T ≤ t < (k + 1) T, n = 2^k n0; data = Append[data, {t, n}], k = k + 1];
  (* reproduction *)
  t = t + dt];

ListPlot[data, AxesLabel → {"Time", "Number of bacteria"},
 LabelStyle → Directive[15]]
```

Out[32]=

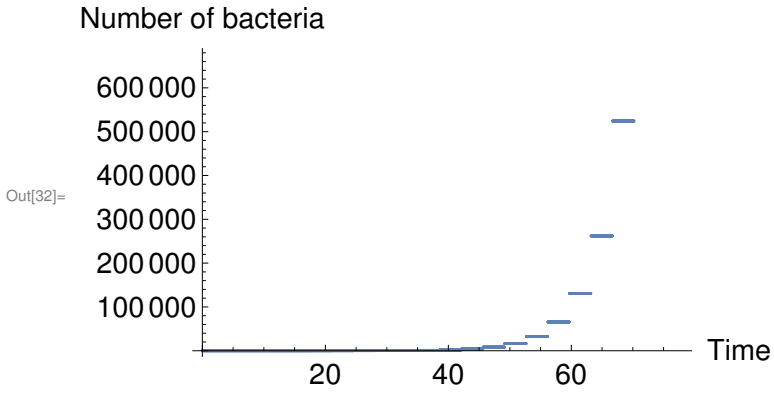

Data fit

In[33]:=
```
Clear[t, k, c, f]

fit = FindFit[data, c^x, c, x] (* data fit *)
```

Out[34]=
```
{c → 1.21336}
```

In[35]:=
```
f[t_] = c^t /. fit;

datafun = Interpolation[data]; (* data vector into a function form *)
```

In[37]:=
```
S = Table[datafun[t] , {t, 0, tMax - 1}]; (* simulated *)
T = Table[f[t], {t, 0, tMax - 1}]; (* theoretical *)

ρr = SpearmanRankTest[S, T, "TestStatistic"] (* Spearsman rank coefficient *)
```

Out[39]=
```
0.998988
```

In[40]:=
```
fit1 = Show[ListPlot[data, AxesLabel → {"Time", "Number of bacteria"},
    LabelStyle → Directive[15]], Plot[c^t /. fit, {t, 0, tMax}, PlotStyle → Pink,
    PlotLegends → {ToString[NumberForm[c /. fit, 4]]^"t"}]] (* plot *)
```

Out[40]=

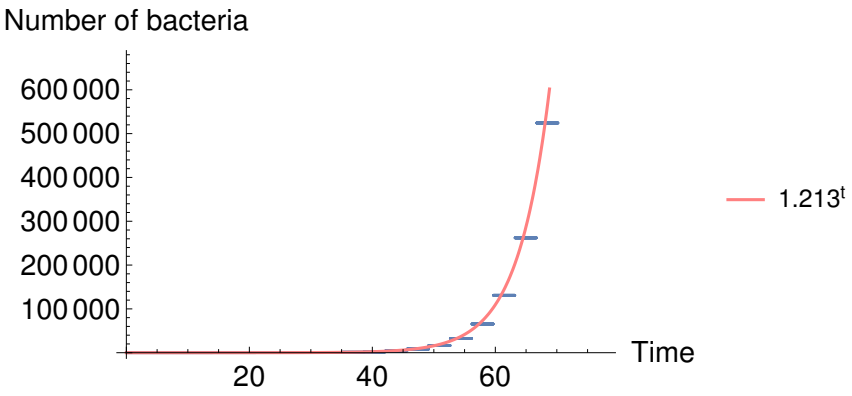

A2 Mitosis controlled by the consumption of a single nutrient

Simulation of a growth curve and distribution of the mitosis ages of cells feeding off a limited amount of resource, using the model equations 2.9 and 2.12.

```
In[•]:= tMax = 168; (* duration of the experiment *)
n0 = 1; (* initial number of cells *)
μ = 1.5 * 10^-4;(* mean value for λ *)
σ = 2 * 10^-4; (* stardard deviation *)
P = 1;(* protein each cell needs to metabolize to reproduce *)

r = 10^3;(* initial available resources *)
Δt = 0.1;(* time steps *)

p = ConstantArray[0, n0];(* protein metabolized by each cell so far *)
a = ConstantArray[0, n0];(* age of each cell *)
n[p_] := Length[p];(* number of cells *)
A = {};(* duration of mitosis for each cell *)
t = 0;(* start experiment *)
data = {{t, n[p]}}; (* starting time and number of cells *)
nutr = {{t, r}};

While[t < tMax,
  {t = t + Δt;
   a = a + Δt;
   λ =
    RandomVariate[TruncatedDistribution[{0, 2 μ}, NormalDistribution[μ, σ]], n[p]]
   (* fraction of nutrients eaten by each cell during a time step *);
   p = p + λ r Δt; (* protein metabolized *)
   r = r - Total[λ] r Δt; (* nutrient still available *)
   Do[
    If[p[[k]] ≥ P, (* condition for division *)
     {p = Flatten[ReplacePart[p, k → {0, 0}]],
      (* divide and reset protein consumption *)
      A = Append[A, a[[k]]], (* save age of mitosis *)
      a = Flatten[ReplacePart[a, k → {0, 0}]](* divide and reset cell ages *)}
    ], {k, n[p]}];
   data = Append[data, {t, n[p]}];
   (* save number of cells in each time step *)
   nutr = Append[nutr, {t, r}](* save amount of nutrient in each time step *)
  }
 ];
```

A3 Data from the first experiment

Growth curves of the cultures of E. coli grown in the IGC lab on different concentrations of glucose. The Optical Densities of the E.coli cultures in minimal media and glucose, measured in the bioscreen can be consulted in the following link: https://drive.google.com/file/d/1Iq95hOOiOPm3JJ-YNLbbqnGVOpqIC_Hq/view?usp=sharing&export=download.

	Culture 1	Culture 2	Culture 3
Sample 1	0.615	0.628	0.753
Sample 2	0.799	1.029	0.891
Sample 3	0.723	0.809	0.773
Average	0.665	0.906	0.768

Table 1: Optical Densities of the pre-cuture read in the multiskan

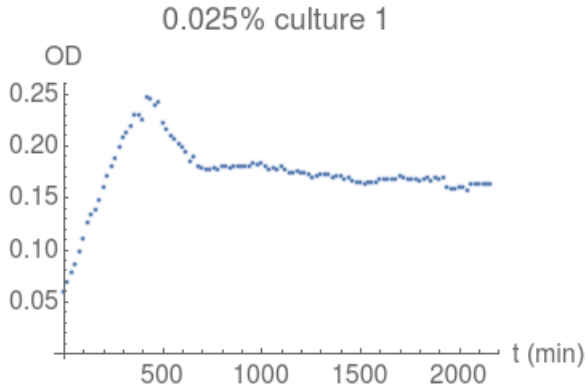

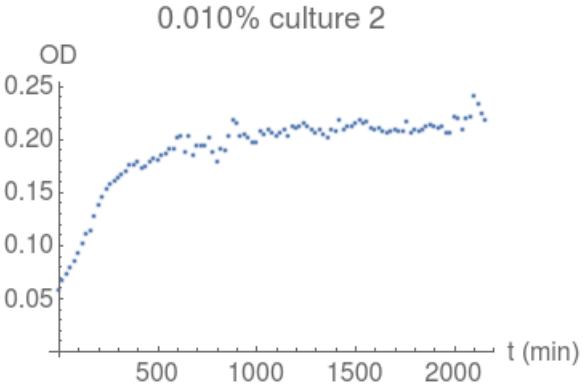

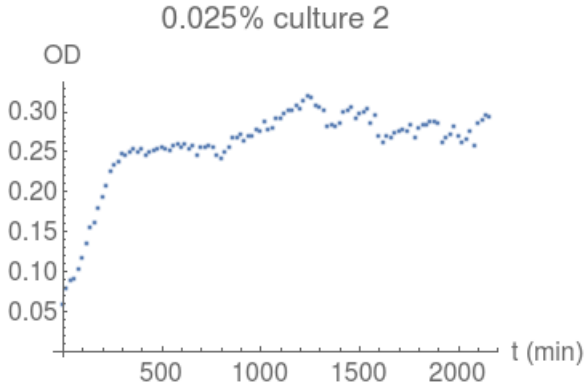

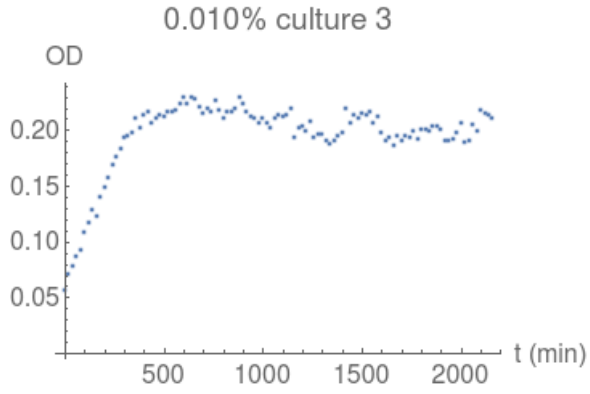

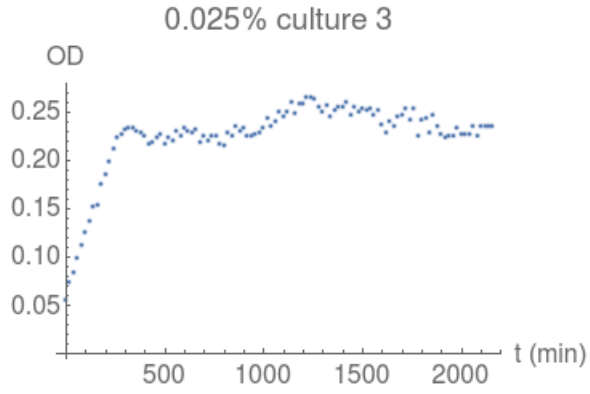

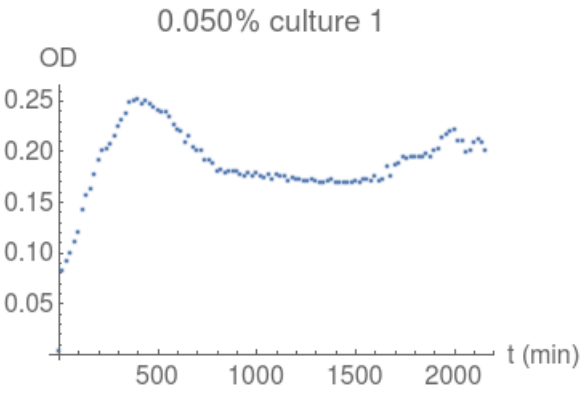
0.050% culture 1
OD
0.25
0.20
0.15
0.10
0.05
500
1000
1500
2000
t (min)

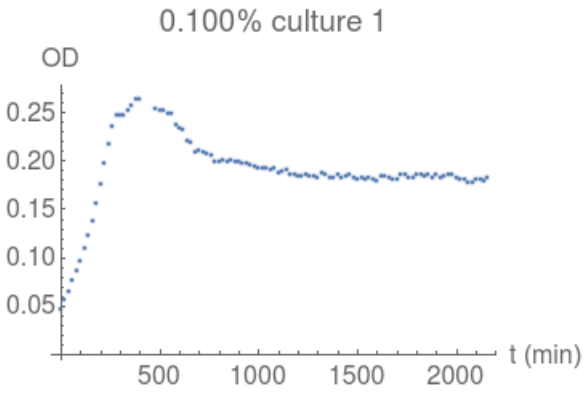
0.100% culture 1
OD
0.25
0.20
0.15
0.10
0.05
500
1000
1500
2000
t (min)

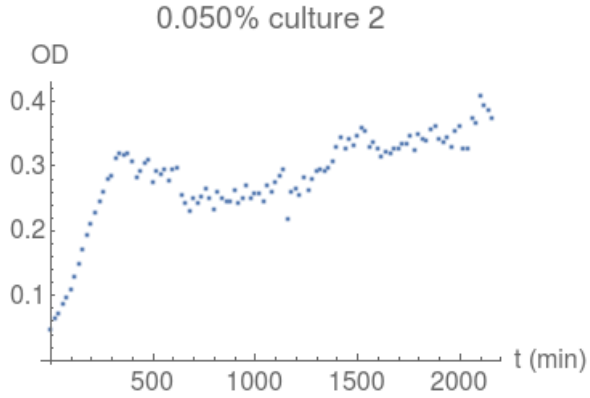
0.050% culture 2
OD
0.4
0.3
0.2
0.1
500
1000
1500
2000
t (min)

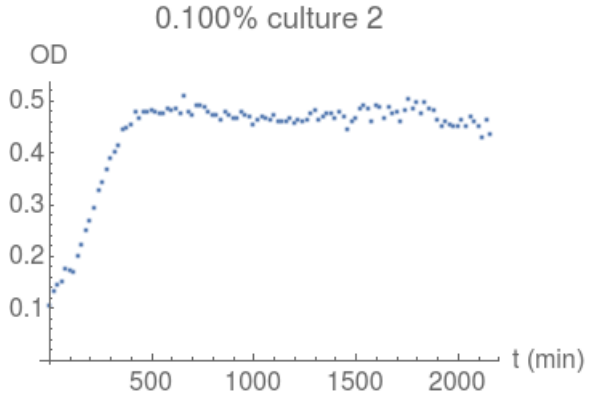
0.100% culture 2
OD
0.5
0.4
0.3
0.2
0.1
500
1000
1500
2000
t (min)

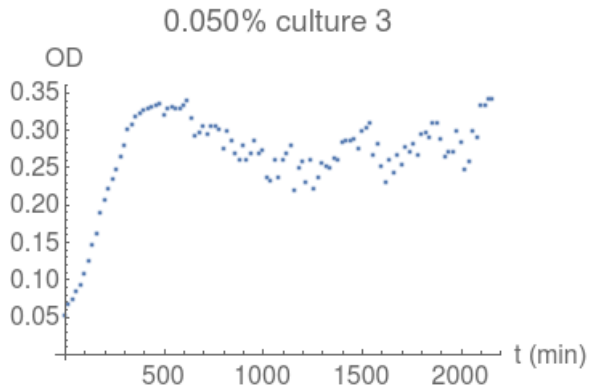
0.050% culture 3
OD
0.35
0.30
0.25
0.20
0.15
0.10
0.05
500
1000
1500
2000
t (min)

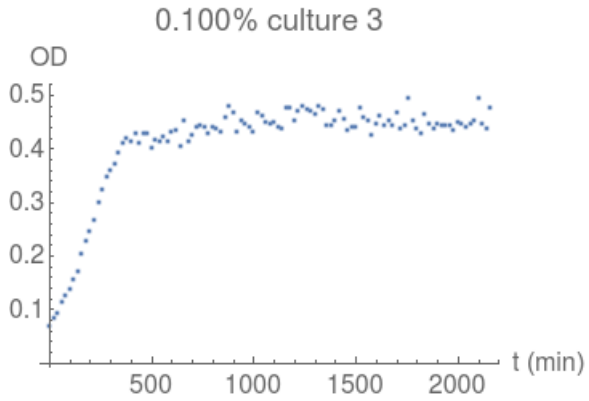
0.100% culture 3
OD
0.5
0.4
0.3
0.2
0.1
500
1000
1500
2000
t (min)

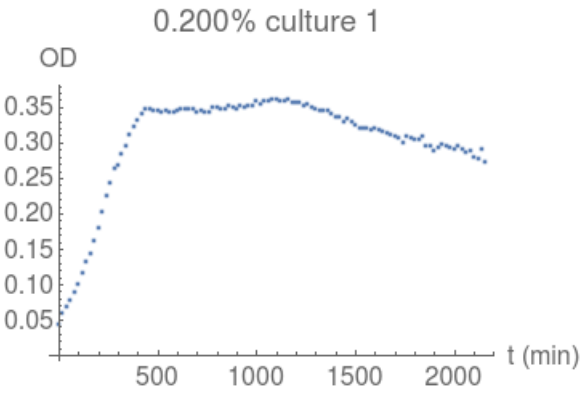
0.200% culture 1
OD
0.35
0.30
0.25
0.20
0.15
0.10
0.05
500
1000
1500
2000
t (min)

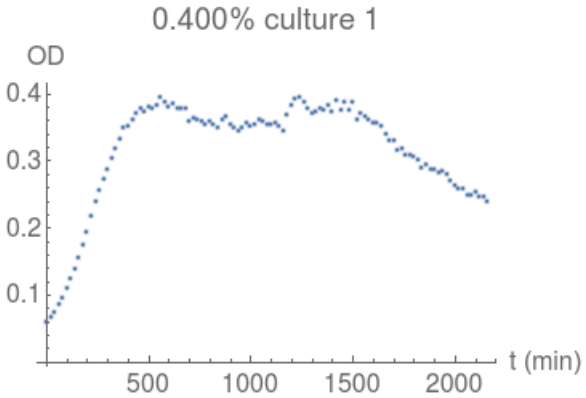
0.400% culture 1
OD
0.4
0.3
0.2
0.1
500
1000
1500
2000
t (min)

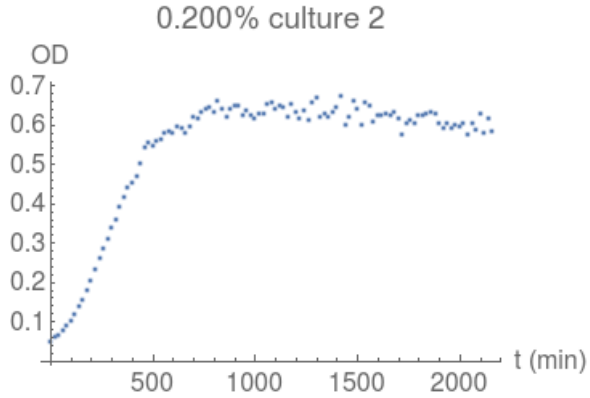
0.200% culture 2
OD
0.7
0.6
0.5
0.4
0.3
0.2
0.1
500
1000
1500
2000
t (min)

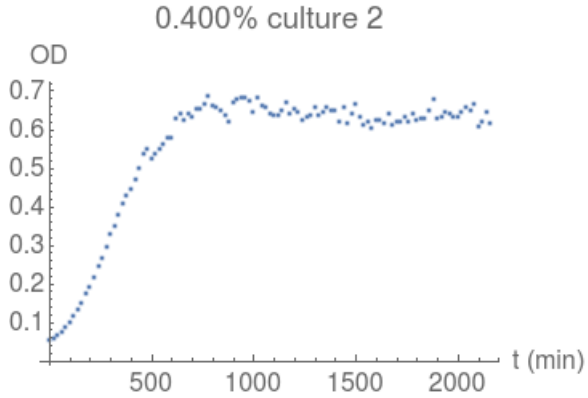
0.400% culture 2
OD
0.7
0.6
0.5
0.4
0.3
0.2
0.1
500
1000
1500
2000
t (min)

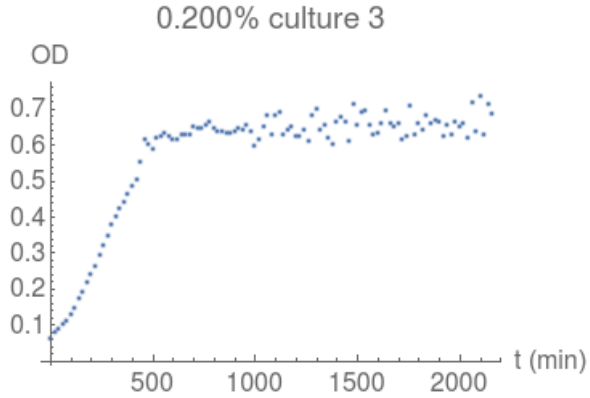
0.200% culture 3
OD
0.7
0.6
0.5
0.4
0.3
0.2
0.1
500
1000
1500
2000
t (min)

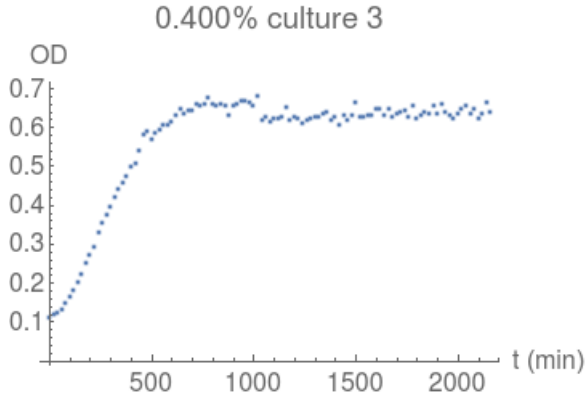
0.400% culture 3
OD
0.7
0.6
0.5
0.4
0.3
0.2
0.1
500
1000
1500
2000
t (min)

A4 Fitting the data from the first experiment with the Monod function

Fitting with the Monod function, of the Optical Densities of one of the E. coli cultures grown in minimal media and 0.100% glucose, measured in the bioscreen.

Experimental data

In[1]:=
```
OD = {0.104, 0.132, 0.145, 0.149, 0.175, 0.172, 0.169, 0.201, 0.221,
    0.250, 0.268, 0.293, 0.326, 0.343, 0.366, 0.389, 0.400, 0.414, 0.443,
    0.446, 0.454, 0.478, 0.466, 0.479, 0.479, 0.481, 0.477, 0.475, 0.476,
    0.483, 0.480, 0.485, 0.476, 0.509, 0.478, 0.472, 0.491, 0.490, 0.486,
    0.479, 0.471, 0.470, 0.463, 0.477, 0.470, 0.464, 0.464, 0.479, 0.470,
    0.469, 0.453, 0.462, 0.469, 0.465, 0.462, 0.472, 0.459, 0.458, 0.460,
    0.466, 0.456, 0.462, 0.460, 0.462, 0.475, 0.480, 0.463, 0.469, 0.476,
    0.474, 0.466, 0.477, 0.468, 0.444, 0.459, 0.465, 0.485, 0.491, 0.483,
    0.460, 0.490, 0.488, 0.466, 0.486, 0.476, 0.479, 0.460, 0.482, 0.503,
    0.484, 0.495, 0.474, 0.496, 0.485, 0.480, 0.462, 0.449, 0.458, 0.452,
    0.450, 0.449, 0.462, 0.449, 0.468, 0.460, 0.450, 0.427, 0.461, 0.435};

tMax = 2160;
time = {0};
Do[time = Append[time, 20 i], {i, 1, tMax/20}];
data = {};
Do[data = Append[data, {time[[i]], OD[[i]]}], {i, 1, Length[OD]}]
T = 600;
DataForFit = {};
For[i = 1, time[[i]] < T, i++,
 DataForFit = Append[DataForFit, data[[i]]]]
ListPlot[{data, DataForFit}, PlotRange → All, GridLines → {{T}},
 TicksStyle → Directive[FontSize → 15], ImageSize → Medium,
 AxesLabel → {Style["t (min)", 15], Style["OD", 15]}]
```

Out[10]=

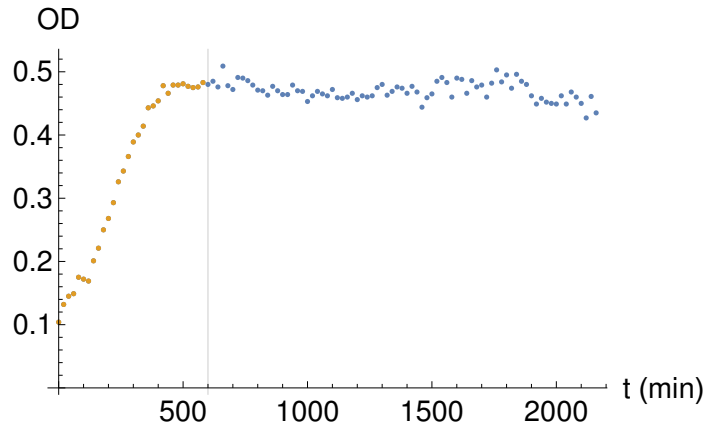

Manual fit

In[11]:=
```
Manipulate[
 Clear[n];
 n[t_] = n[t] /.
   NDSolve[{n'[t]/n[t] == g0 (R0 + k (n0 - n[t]))/(R12 + R0 + k (n0 - n[t])), n[0] == n0}, n, {t, 0, T}][[1, 1]];
 χ2 = Sum[(OD[[i]] - n[time[[i]]])^2/n[time[[i]]], {i, T/20 + 0.5}];

 Show[Plot[n[t], {t, 0, T}, PlotStyle → Pink,
   AxesLabel → {Style["t", 15], Style["OD", 15]},
   TicksStyle → Directive[FontSize → 15], PlotRange → {0, Max[OD]}],
  ListPlot[DataForFit]],

 {{n0, 0.11}, 0.08, 0.15},
 {{R0, 0.37}, 0.1, 1},
 {{R12, 0.140}, 0.001, 1},
 {{g0, 0.0067}, 0.0001, 0.01},
 {{k, 0.99}, 0.1, 3},
 TrackedSymbols :> True]
```

Out[11]=

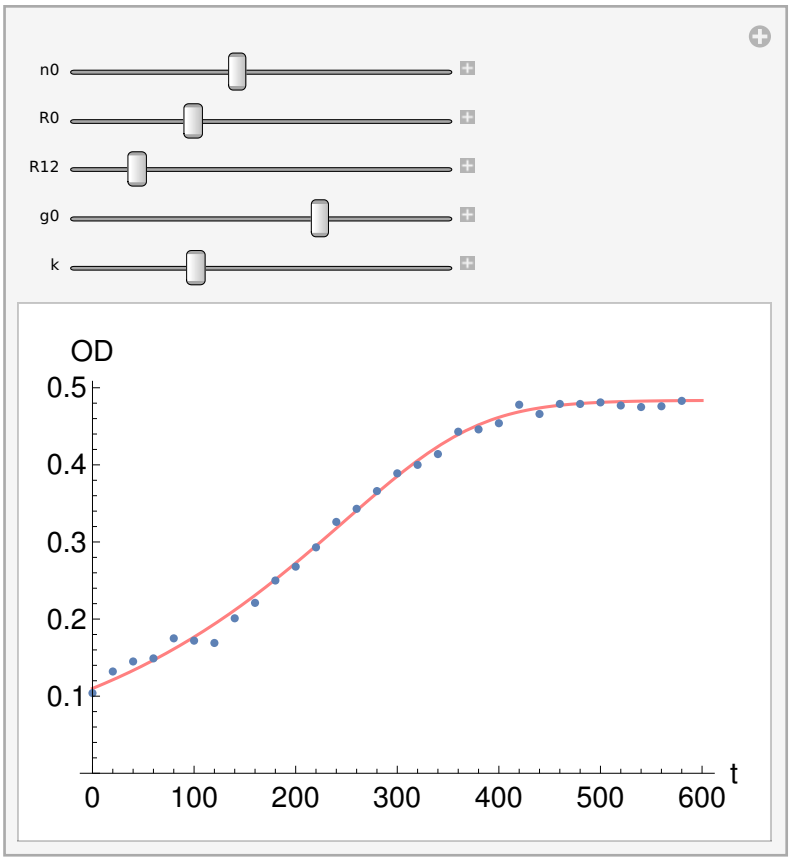

Fit using the method of random variables

```
For[j = 1, j < 10^4, j++,
  n0rand = RandomReal[{0.08, 0.15}];
  R0rand = RandomReal[{0.1, 1}];
  R12rand = RandomReal[{0.01, 1}];
  g0rand = RandomReal[{0.0001, 0.1}];
  krand = RandomReal[{0.1, 5}];

  Clear[nRand];
  nRand[t_] = nRand[t] /.
    NDSolve[{nRand'[t]/nRand[t] == g0rand (R0rand + krand (n0rand - nRand[t]))/(R12rand + R0rand + krand (n0rand - nRand[t])),
      nRand[0] == n0rand}, nRand, {t, 0, T}][[1, 1]];

  Newχ2 = Sum[(OD[[i]] - nRand[time[[i]]])^2/nRand[time[[i]]], {i, T/20 + 0.5}];

  If[0 < Newχ2 < χ2, χ2 = Newχ2;
   n[t_] = nRand[t]; n0 = n0rand; R0 = R0rand; R12 = R12rand; g0 = g0rand; k = krand;
   Abort[]];
 ];

datafun = Interpolation[DataForFit];
exp = Table[datafun[t] , {t, 0, 580}];
teor = Table[n[t], {t, 0, 580}];

ρr = SpearmanRankTest[exp, teor, "TestStatistic"];

Show[Plot[n[t], {t, 0, T}, PlotStyle → Pink,
  AxesLabel → {Style["t (min)", 15], Style["OD", 15]},
  TicksStyle → Directive[FontSize → 15], PlotRange → {{0, T - 10}, {0, 0.59}}],
 ListPlot[DataForFit, ImageSize → Medium, PlotRange → All]]

Print["χ2 = ", χ2, "\nρr = ", ρr, "\n OD₀ = ", n0, "\n R₀ = ",
 R0, "\n R₁/₂ = ", R12, "\n g₀ = ", g0, "\n k = ", k, "\n"]
```

Out[•]=

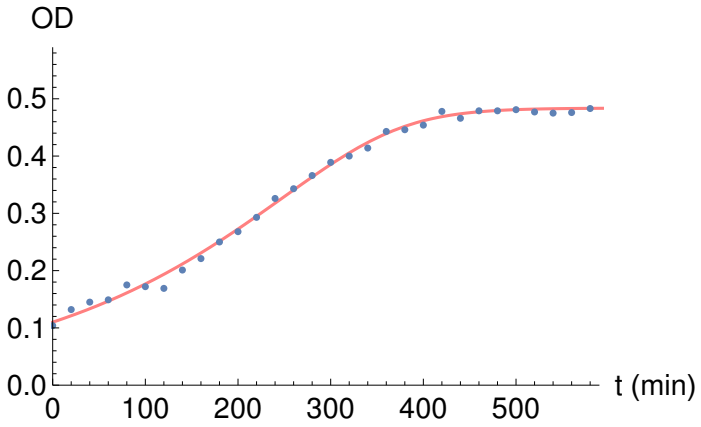

$\chi 2$ = 0.00923344
ρr = 0.981368
OD_0 = 0.108482
R_0 = 0.540954
$R_{1/2}$ = 0.519862
g_0 = 0.0081962
k = 1.42897

Results of another 5 fits done with the Monod function:

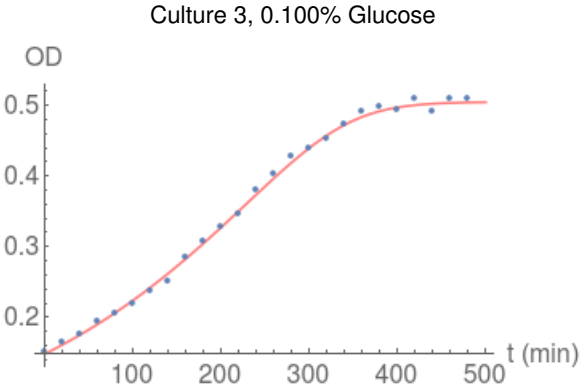

$\chi 2$ = 0.00222884
ρr = 0.994047
OD_0 = 0.147679
R_0 = 0.170954
$R_{1/2}$ = 0.0447619
g_0 = 0.00535898
k = 0.478175

Culture 2, 0.200% Glucose

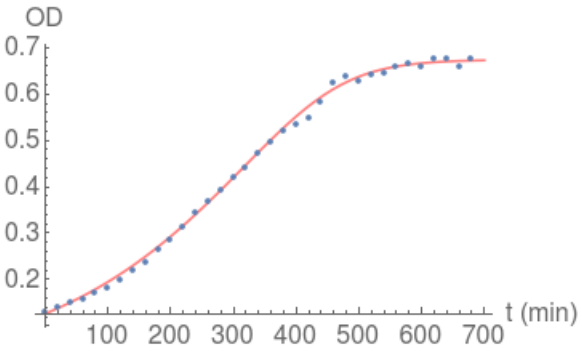

$\chi 2$ = 0.00812889
ρr = 0.994288
OD_0 = 0.126122
R_0 = 0.279187
$R_{1/2}$ = 0.126696
g_0 = 0.00643404
k = 0.509476

Culture 3, 0.200% Glucose

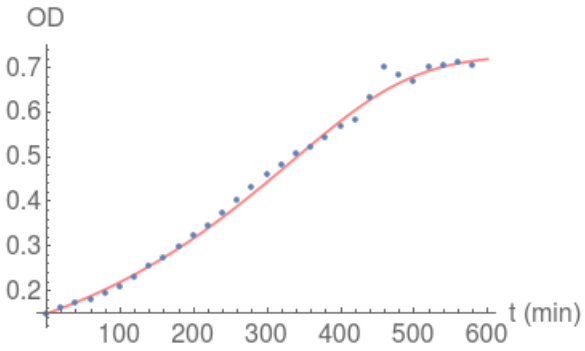

$\chi 2$ = 0.00979845
ρr = 0.99747
OD_0 = 0.148235
R_0 = 0.271918
$R_{1/2}$ = 0.103689
g_0 = 0.00548156
k = 0.468202

Culture 2, 0.400% Glucose

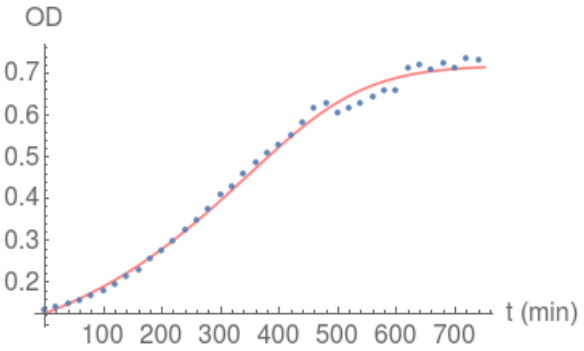

$\chi 2$ = 0.0157017
ρr = 0.996282
OD_0 = 0.126187
R_0 = 0.205928
$R_{1/2}$ = 0.125242
g_0 = 0.0067464
k = 0.347402

Culture 3, 0.400% Glucose

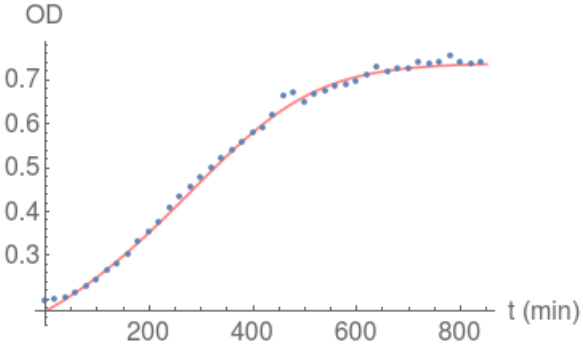

$\chi 2$ = 0.00992542
ρr = 0.995742
OD_0 = 0.172213
R_0 = 0.243744
$R_{1/2}$ = 0.227964
g_0 = 0.00750602
k = 0.430203

A5 Fitting the data from the first experiment with the logistic function obtained with the Mass Action Law

Fitting with the logistic function obtained with the Mass Action Law, of the Optical Densities of one of the E. coli cultures grown in minimal media and 0.100% glucose, measured in the bioscreen.

Experimental data

In[1]:=
```
OD = {0.104, 0.132, 0.145, 0.149, 0.175, 0.172, 0.169, 0.201, 0.221,
    0.250, 0.268, 0.293, 0.326, 0.343, 0.366, 0.389, 0.400, 0.414, 0.443,
    0.446, 0.454, 0.478, 0.466, 0.479, 0.479, 0.481, 0.477, 0.475, 0.476,
    0.483, 0.480, 0.485, 0.476, 0.509, 0.478, 0.472, 0.491, 0.490, 0.486,
    0.479, 0.471, 0.470, 0.463, 0.477, 0.470, 0.464, 0.464, 0.479, 0.470,
    0.469, 0.453, 0.462, 0.469, 0.465, 0.462, 0.472, 0.459, 0.458, 0.460,
    0.466, 0.456, 0.462, 0.460, 0.462, 0.475, 0.480, 0.463, 0.469, 0.476,
    0.474, 0.466, 0.477, 0.468, 0.444, 0.459, 0.465, 0.485, 0.491, 0.483,
    0.460, 0.490, 0.488, 0.466, 0.486, 0.476, 0.479, 0.460, 0.482, 0.503,
    0.484, 0.495, 0.474, 0.496, 0.485, 0.480, 0.462, 0.449, 0.458, 0.452,
    0.450, 0.449, 0.462, 0.449, 0.468, 0.460, 0.450, 0.427, 0.461, 0.435};

tMax = 2160;
Δt = 20;
time = {0};
Do[time = Append[time, 20 i], {i, 1, tMax/Δt}];
data = {};
Do[data = Append[data, {time[[i]], OD[[i]]}], {i, 1, Length[OD]}]
T = 600;
DataForFit = {};
For[i = 1, time[[i]] < T, i++,
 DataForFit = Append[DataForFit, data[[i]]]]
ListPlot[{data, DataForFit}, PlotRange → All,
 GridLines → {{T}}, AxesLabel → {Style["t (min)", 15], Style["OD", 15]},
 TicksStyle → Directive[FontSize → 15], ImageSize → Medium]
```

Out[11]=

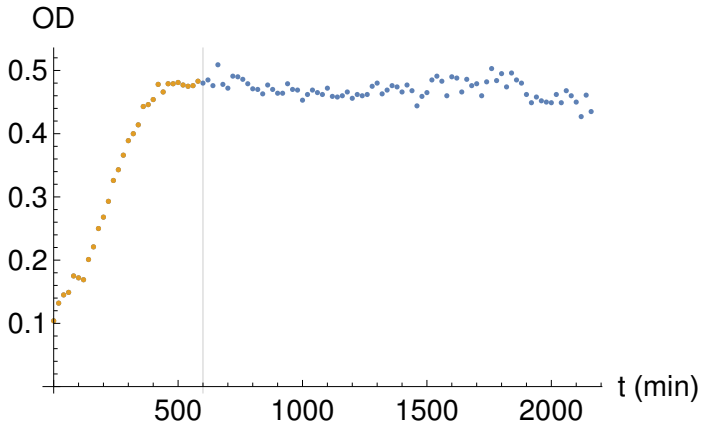

FindFit

In[12]:=
```
Clear[f0, b, m, t]

f[t_] = m E^(b m t) / (m/f0 - 1 + E^(b m t))

fit = FindFit[DataForFit, f[t], {f0, b, m}, t]

χ2 = Sum[(datafun[t] - f[t] /. fit)^2 / (f[t] /. fit), {t, 580}];

datafun = Interpolation[DataForFit];(* data vector into a function form *)
exp = Table[datafun[t] , {t, 0, 580}];(* simulated *)

teor = Table[f[t] /. fit, {t, 0, 580}];(* theoretical *)
ρr = SpearmanRankTest[exp, teor, "TestStatistic"];
(* Spearsman rank coefficient *)

Print["χ2 = ", χ2, "\nρr = ", ρr, "\n"]

Show[ListPlot[DataForFit,
  AxesLabel → {"t (min)", "OD"}, LabelStyle → Directive[15]],
 Plot[f[t] /. fit, {t, 0, T}, PlotStyle → Pink]]
```

Out[13]=
$$\frac{e^{b\,m\,t}\,m}{-1+e^{b\,m\,t}+\frac{m}{f0}}$$

Out[14]=
$$\{f0 \to 0.0941713,\ b \to 0.0165668,\ m \to 0.512274\}$$

```
χ2 = 0.491217
ρr = 0.981368
```

Out[21]=

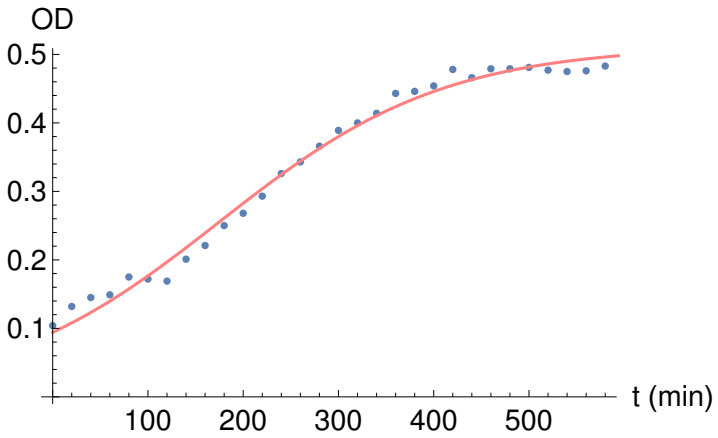

Manual fit

In[22]:=
```
Clear[f, f0, b, m, t]

Manipulate[
 f[t_] = m E^(b m t) / (m/f0 - 1 + E^(b m t));
 χ2 = Sum[(datafun[i] - f[i])^2 / f[i], {i, 580}];

 Show[Plot[f[t], {t, 0, 580},
   AxesLabel → {Style["t", 15], Style["OD", 15]}, PlotStyle → Pink,
   TicksStyle → Directive[FontSize → 15], PlotRange → {0, f[580] + 0.1}],
  ListPlot[DataForFit]],

 {{f0, 0.1}, 0.01, 1},
 {{b, 0.0161}, 0.001, 0.1},
 {{m, 0.513}, 0.01, 1},

 TrackedSymbols :> True]
```

Out[23]=

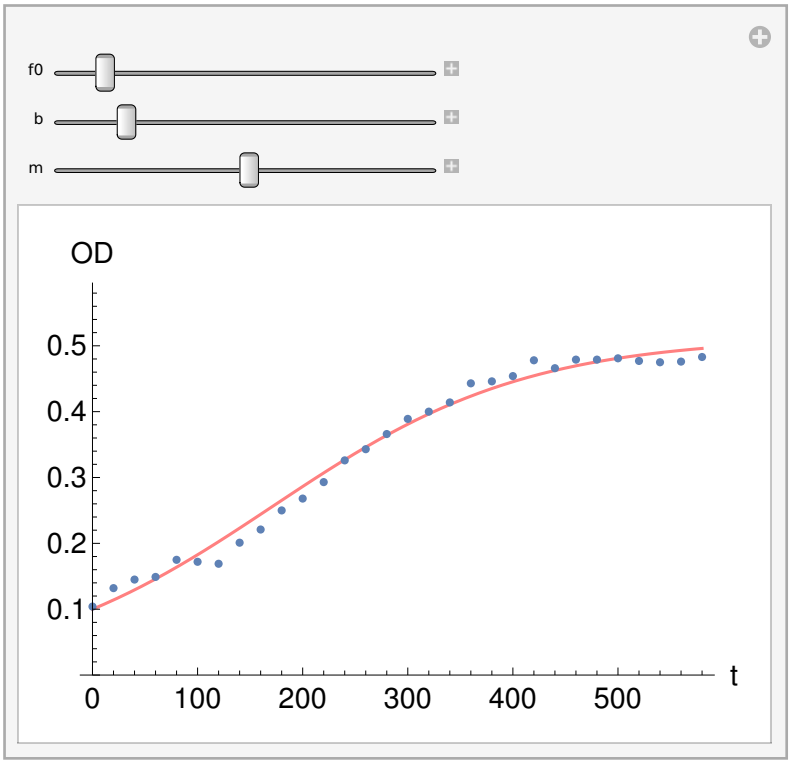

In[24]:=
```
χ2
```

Out[24]=
```
0.452875
```

Random variables method

In[49]:=
```
Clear[f]

For[j = 1, j < 10^4, j++,
 f0Rand = RandomReal[{0.08, 0.15}];
 bRand = RandomReal[{0.009, 0.02}];
 mRand = RandomReal[{0.4, 0.65}];
 f[t_] = mRand E^(bRand mRand t) / (mRand/f0Rand - 1 + E^(bRand mRand t));
 Newχ2 = Sum[(datafun[t] - f[t])^2 / f[t], {t, 580}];
 teor = Table[f[t] /. fit, {t, 0, 580}]; (* theoretical *)
 newρr = SpearmanRankTest[exp, teor, "TestStatistic"];
 (* Spearsman rank coefficient *)

 If[0 < Newχ2 < χ2, χ2 = Newχ2;
  ρr = newρr;
  f0 = f0Rand; b = bRand;
  m = mRand;
  Abort[]];
]

Show[ListPlot[DataForFit,
  AxesLabel → {"t (min)", "OD"}, LabelStyle → Directive[15]],
 Plot[f[t] /. fit, {t, 0, T}, PlotStyle → Pink]]

Print["χ2 = ", χ2, "\nρr = ", ρr, "\n f0 = ", f0, "\n b = ", b, "\n m = ", m, "\n"]
```

Out[47]=

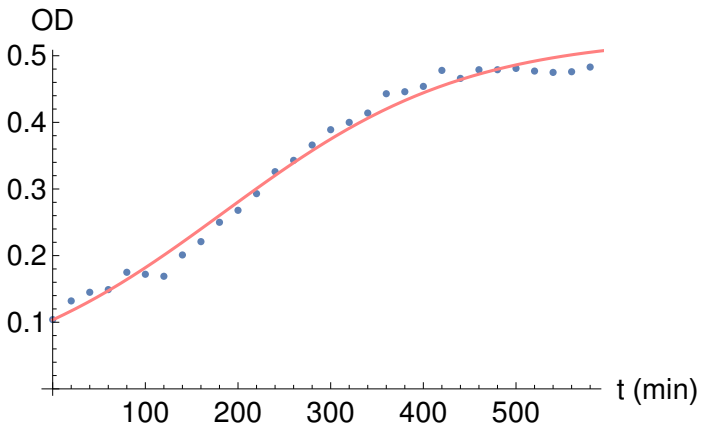


```
χ2 = 0.414907
ρr = 0.981368
 f0 = 0.103599
 b = 0.0144695
 m = 0.529594
```

Results of another 5 fits done with the Monod function:

Culture 3, 0.100% Glucose

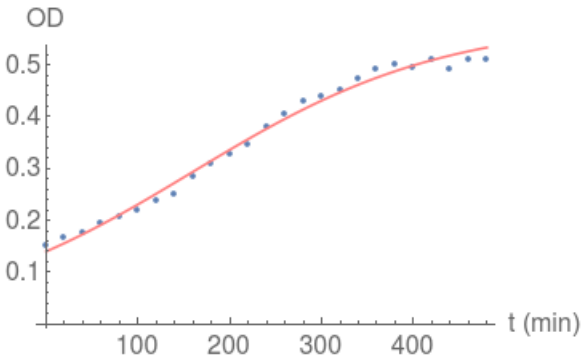

$\chi 2$ = 0.183946
ρr = 0.994047
OD_0 = 0.139671
b = 0.0124974
m = 0.584166

Culture 2, 0.200% Glucose

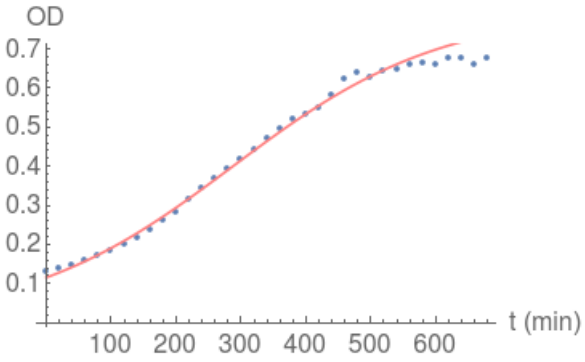

$\chi 2$ = 0.173501
ρr = 0.999138
OD_0 = 0.115182
b = 0.00776496
m = 0.798383

Culture 3, 0.200% Glucose

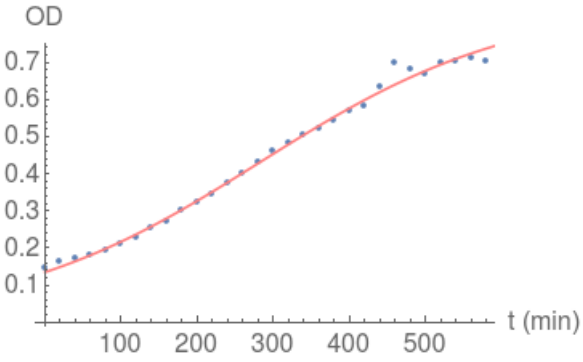

$\chi 2$ = 0.212626
ρr = 0.99747
OD_0 = 0.134427
b = 0.00693547
m = 0.861874

Culture 2, 0.400% Glucose

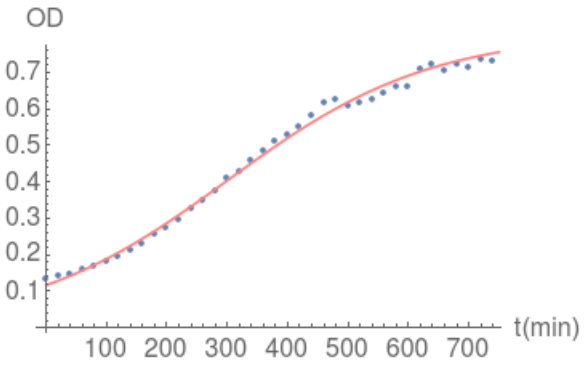

$\chi 2$ = 0.278691
ρr = 0.996461
OD_0 = 0.116091
b = 0.00734733
m = 0.808147

Culture 3, 0.400% Glucose

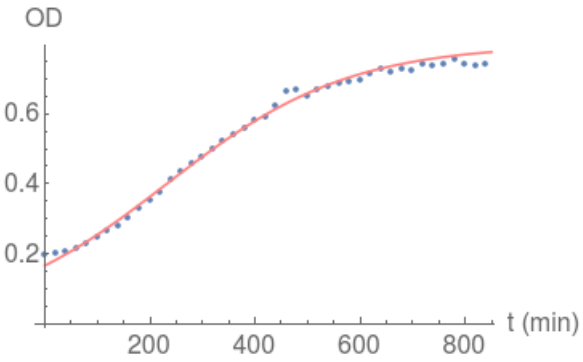

$\chi 2$ = 0.212555
ρr = 0.997345
OD_0 = 0.165661
b = 0.00724938
m = 0.797909